ATTACHMENT 0026

AMSAA Planning Model Based on Projection Methodology (PM2)

May 2006

TECHNICAL REPORT NO. TR-2006-9

PLANNING MODEL BASED ON PROJECTION METHODOLOGY (PM2)

- MAY 2006 -

APPROVED FOR PUBLIC RELEASE; DISTRIBUTION IS UNLIMITED.

U.S. ARMY MATERIEL SYSTEMS ANALYSIS ACTIVITY
ABERDEEN PROVING GROUND, MARYLAND 21005-5071

DESTRUCTION NOTICE

Destroy by any method that will prevent disclosure of contents or reconstruction of the document.

DISCLAIMER

The findings in this report are not to be construed as an official Department of the Army position unless so specified by other official documentation.

WARNING

Information and data contained in this document are based on the input available at the time of preparation.

TRADE NAMES

The use of trade names in this report does not constitute an official endorsement or approval of the use of such commercial hardware or software. The report may not be cited for purposes of advertisement.

REPORT DOCUMENTATION PAGE

Form Approved
OMB No. 0704-0188

Public reporting burden for this collection of information is estimated to average 1 hour per response, including the time for reviewing instructions, searching existing data sources, gathering and maintaining the data needed, and completing and reviewing the collection of information. Send comments regarding this burden estimate or any other aspect of this collection of information, including suggestions for reducing the burden to Washington Headquarters Services, Directorate for Information Operations and Reports, 1215 Jefferson Davis Highway, Suite 1204, Arlington, VA 22202-4302, and to the Office of Management and Budget, Paperwork Reduction Project (0704-0188), Washington, DC 20503.

1. AGENCY USE ONLY (LEAVE BLANK)	2. REPORT DATE	3. REPORT TYPE AND DATES COVERED
	May 2006	Technical Report

4. TITLE AND SUBTITLE
Planning Model based on Projection Methodology (PM2)

5. FUNDING NUMBERS

6. AUTHOR(S)
Paul M. Ellner, and J. Brian Hall

7. PERFORMING ORGANIZATION NAME(S) AND ADDRESS(ES)
Director; U.S. Army Materiel Systems Analysis Activity
AMSRD-AMS-LA
392 Hopkins Road
Aberdeen Proving Ground, MD 21005-5071

8. PERFORMING ORGANIZATION REPORT NUMBER
TR-2006-9

9. SPONSORING/MONITORING AGENCY NAME(S) AND ADDRESS(ES)
Director; U.S. Army Materiel Systems Analysis Activity
AMSRD-AMS-LA
392 Hopkins Road
Aberdeen Proving Ground, MD 21005-5071

10. SPONSORING/MONITORING AGENCY REPORT NUMBER

11. SUPPLEMENTARY NOTES

12a. DISTRIBUTION/AVAILABILITY STATEMENT
Approved for public release; distribution is unlimited.

12b. DISTRIBUTION CODE
N/A

13. ABSTRACT (Maximum 200 words)

14. SUBJECT TERMS
Reliability growth planning.

15. NUMBER OF PAGES

16. PRICE CODE
N/A

17. SECURITY CLASSIFICATION OF REPORT	18. SECURITY CLASSIFICATION OF THIS PAGE	19. SECURITY CLASSIFICATION OF ABSTRACT	20. LIMITATION OF ABSTRACT
Unclassified.	Unclassified.	Unclassified.	Same as report.

NSN 7540-01-280-5500

Standard Form 298 (Rev. 2-89)
Prescribed by ANSI Std. Z39-18
298-102

THIS PAGE INTENTIONALLY LEFT BLANK.

TABLE OF CONTENTS

PAGE

ACKNOWLEDGEMENTS ..... **vii**
LIST OF ACRONYMS ..... **ix**
LIST OF NOTATION ..... **xi**
LIST OF DEFINITIONS ..... **viii**
LIST OF FIGURES ..... **xv**
LIST OF TABLES ..... **xv**

1. EXECUTIVE SUMMARY **1**
1.1 The Planning Model based on Projection Methodology (PM2) 1
1.2 PM2 Assumptions 1
1.3 PM2 Limitations 1
1.4 PM2 Benefits 1
1.5 Overview 2

2. INTRODUCTION **3**
2.1 Background 3
2.2 Purpose 3
2.3 Study Overview 3

3. MIL-HDBK-189 IDEALIZED GROWTH CURVE **5**
3.1 Background 5
3.2 Depicting the Planned Reliability Growth 5
3.3 MIL-HDBK-189 Planning Model Issues 6

4. DERIVED RELIABILITY GROWTH PATTERNS **8**
4.1 Assumptions 8
4.2 Background Information 8
4.3 Parsimonious Approximations 9
4.3.1 Expected Number of Modes and its Derivative 9
4.3.2 Expected System Failure Intensity and MTBF 11

5. SIMULATION **13**
5.1 Simulation Overview 13
5.2 Simulation Results 13

6. USING PLANNING PARAMETERS **17**
6.1 Methodology 17
6.1.1 Planning Formulae not Using Mode Classification 17
6.1.2 Planning Formulae Using Mode Classification 18
6.2 Comparisons of MTBF Approximations 19
6.2.1 Gamma Parent Population 20
6.2.2 Lognormal Parent Population 21
6.2.3 Geometric Initial Mode Failure Rates 23

7. RELIABILITY GROWTH POTENTIAL 26
7.1 Growth Potential in Terms of Planning Parameters 26
7.2 Planning Parameter β in Terms of Growth Potential.....26
7.3 Plausibility Metrics for Planning Parameters 26

8. GENERATING A PLANNED RELIABILITY GROWTH PATH 29

REFERENCES.....31

APPENDIX A - SIMULATION A-1
A.1 Simulating a Developmental Test A-3
A.2 Replicating the Simulation..... A-5
A.3 Input Parameters, and Distributions..... A-6
A.4 Visual Growth Suite..... A-8
A.5 Average Number of Failure Modes Surfaced A-10
A.6 Failure Mode Profile A-12
A.7 Cumulative Failure Mode Profile A-13
A.8 System Mean Time Between Failure A-14
A.9 System Failure Intensity..... A-17
A.10 The Rate of Occurrence of Unseen Failure Modes..... A-18
A.11 System MTBF based on Planning Parameters..... A-18

APPENDIX B – DISTRIBUTION LIST B-1

ACKNOWLEDGEMENTS

The U.S. Army Materiel System Analysis Activity (AMSAA) recognizes the following individuals for their contributions to this report.

The authors are:

Paul M. Ellner, Logistics Analysis Division.
J. Brian Hall, Logistics Analysis Division.

Appreciation is extended to David Mortin, Logistics Analysis Division, for critical comments and assessment of this report.

THIS PAGE IS INTENTIONALLY LEFT BLANK.

LIST OF ACRONYMS

AMSAA	-	Army Materiel Systems Analysis Activity
CAP	-	Corrective Action Period
DAMF	-	Defense Acquisition Management Framework
DoD	-	Department of Defense
FEF	-	Fix Effectiveness Factor
FOT	-	First Occurrence Time
IOT&E	-	Initial Operational Test and Evaluation
MIL-HDBK	-	Military Handbook
MLE	-	Maximum Likelihood Estimate/Estimation
MS	-	Management Strategy
MTBF	-	Mean Time Between Failure
OMS/MP	-	Operational Mode Summary/Mission Profile
PDF	-	Probability Density Function
PM2	-	Planning Model based on Projection Methodology
RAM	-	Reliability, Availability, and Maintainability
SDD	-	System Development and Demonstration

THIS PAGE IS INTENTIONALLY LEFT BLANK.

LIST OF NOTATION

k – total number of potential failure modes.
m – number of surfaced failure modes.
T – total duration of a developmental test.
$N_M(t)$ *- number of failures by t for MIL-HDBK-189 model.*
$\rho_M(t)$ *- failure intensity for MIL-HDBK-189 model.*
t_1 *– length of the initial test phase.*
M_1 *– average initial MTBF over* t_1*.*
M_G *– goal MTBF.*
α_M *– growth rate.*
ϕ_i *- average failure rate for test phase i.*
MS – management strategy.
μ_d *– average fix effectiveness.*
$M(t)$ *- number of modes surfaced by time t.*
$\mu(t)$ *- expected value of* $M(t)$.
$\mu_k(t)$ *- approximation of* $\mu(t)$.
$\Lambda_U(t)$ *- system failure intensity for unsurfaced modes.*
$\Lambda(t)$ *- system failure intensity, after mode mitigation.*
N_i *– number of failures for failure mode i.*
N – the total number of failures (for all modes).
λ *– initial system failure intensity.*
λ_i *– true but unknown initial failure rate for mode i.*
$\hat{\lambda}_i$ *- standard estimate of* λ_i.
$\tilde{\lambda}_i$ *- the Stein estimate of* λ_i.
θ_S *- true but unknown Stein shrinkage factor.*
$h(t)$ *- expected rate of occurrence of new modes at time t.*
$h_k(t)$ *- approximation of* $h(t)$.
d_i *- true but unknown fix effectiveness for mode i.*
$\rho(t)$ *- expected failure intensity at time t.*
$\rho_k(t)$ *- approximation of* $\rho(t)$.
$MTBF(t)$ *- MTBF at time t.*
$MTBF_k(t)$ *- approximation of* $MTBF(t)$.

THIS PAGE IS INTENTIONALLY LEFT BLANK.

LIST OF DEFINITIONS

1. **A-Mode** – a failure mode that will not be addressed via corrective action.

2. **B-Mode** – a failure mode that will be addressed via corrective action, if surfaced.

3. **Fix Effectiveness Factor** – fraction reduction in an initial failure mode rate of occurrence due to implementation of corrective action.

4. **Management Strategy** – the fraction of the initial system failure intensity that is planned to be addressed via corrective action.

5. **Repeat** – a failure mode with two or more associated failures.

THIS PAGE IS INTENSIONALLY LEFT BLANK.

LIST OF FIGURES

No.	Title	Page
1	Average Number of Surfaced Modes (Loglogistic)	15
2	Reciprocal of the Failure Intensity (Loglogistic)	15
3	Average Number of Surfaced Modes (Geometric)	15
4	Reciprocal of the Failure Intensity (Geometric)	16
5	Reciprocal of the Failure Intensity (Gamma)	21
6	Reciprocal of the Failure Intensity (Log Normal)	21
7	Top W Failure Modes (Log Normal)	22
8	Reciprocal of the Failure Intensity (Log Normal)	22
9	Top W Failure Modes (Log Normal)	23
10	Reciprocal of the Failure Intensity (Geometric)	24
11	Top W Failure Modes (Geometric)	24
12	PM2 Reliability Growth Planning Curve	28
13	Failure Rate Parent Populations	A-7
14	Average Number of Modes Surfaced	A-12
15	Failure Mode Profile	A-13
16	Cumulative Failure Mode Profile	A-14
17	System MTBF	A-16
18	System Failure Intensity	A-18
19	Portion of the Failure Intensity due to Unobserved Modes	A-19
20	System MTBF based on Planning Parameters	A-19

LIST OF TABLES

No.	Title	Page
1	Visual Growth Suite Parameter MLEs	A-10

THIS PAGE IS INTENTIONALLY LEFT BLANK.

1. EXECUTIVE SUMMARY.

1.1. The Planning Model based on Projection Methodology (PM2).

The U.S. Army Materiel Systems Analysis Activity (AMSAA) has developed a new reliability growth planning model. The new model is referred to as the Planning Model based on Projection Methodology, or PM2. PM2 can: (1) aid in constructing a reliability growth planning curve over a developmental test program useful to program management; (2) serve as a baseline against which reliability assessments can be compared and; (3) highlight the need to management when reallocation of resources is necessary.

1.2. PM2 Assumptions.

There are a number of reasonable assumptions associated with PM2. The first assumption is that there are a large number of potential failure modes. As a rule of thumb, the potential number of failure modes should be at least five times the number of failure modes that are expected to be surfaced during the planned test period. Second, each failure mode time to first occurrence is assumed exponential. Finally, it is assumed that each failure mode occurs independently and causes system failure.

1.3. PM2 Limitations.

All reliability growth planning models have limitations. The first limitation associated with PM2 is that the portion of testing utilized for reliability growth planning should be reflective of the Operation Mode Summary/Mission Profile (OMS/MP). This limitation is not unique to PM2 – it is a limitation associated with all reliability growth planning models. Second, one must postulate a baseline test schedule. That is, one must determine the number of hours, or miles, per unit per month over the test period. Finally, fix implementation periods must be specified within the planned test schedule.

1.4. PM2 Benefits.

There are a number of benefits associated with the new planning model. PM2 is unique in comparison to other reliability growth planning models in that it utilizes planning parameters that are directly influenced by program management. Some of these parameters include: (1) the initial system MTBF; (2) the fraction of the initial failure rate addressable via corrective action (referred to as management strategy); (3) the goal system MTBF; (4) the average fix effectiveness of corrective actions; (5) the duration of developmental testing and; (6) the average delay associated with fix implementation. A second benefit of PM2 is that the model can determine the impact of changes to the planned test schedule, and associated fix implementation periods. Third, PM2's measures of programmatic risk are not sensitive to the length of the initial test phase (which is a limitation of the MIL-HDBK-189 planning model). Finally, PM2 can be applied to programs with limited opportunities for implementation of corrective actions.

1.5. Overview.

In following sections of this report, exact expressions for the expected number of surfaced failure modes and system failure intensity as functions of test time are presented under the assumption that the surfaced modes are mitigated through corrective actions. These exact expressions depend on a large number of parameters. Functional forms are derived to approximate these quantities that depend on only a few parameters. Such parsimonious approximations are suitable for developing reliability growth plans and portraying the associated planned growth path. Simulation results indicate that the functional form of the derived parsimonious approximations can adequately represent the expected reliability growth associated with a variety of patterns for the failure mode initial rates of occurrence. A sequence of increasing MTBF target values can be constructed from the parsimonious MTBF projection approximation based on: (1) planning parameters that determine the parsimonious approximation; (2) corrective action mean lag time with respect to implementation and; (3) the test schedule that gives the number of planned Reliability, Availability, and Maintainability (RAM) test hours per month and specifies corrective action implementation periods.

2. INTRODUCTION.

2.1. Background.

To mature the reliability of a complex system under development it is important to formulate a detailed reliability growth plan. One aspect of this plan is a depiction of how the system's reliability is expected to increase over the developmental test period. The depicted growth path serves as a baseline against which reliability assessments can be compared. Such baseline planning curves for Department of Defense (DoD) systems have frequently been developed in the past utilizing the assumed reliability growth pattern specified in Military Handbook 189 (MIL-HDBK-189) (Department of Defense, 1981). This growth relationship is between the reliability, expressed as the mean test duration between system failures and a continuous measure of test duration such as time or mileage. The equation governing this growth pattern was motivated by the empirically derived linear relationship observed for a number of data sets by Duane (1964), between the developmental system cumulative failure rate and the cumulative test time when plotted on a log-log scale.

2.2. Purpose.

In this paper we obtain a non-empirical relationship between the mean test duration between system failures and cumulative test duration that can be utilized for reliability growth planning. This relationship is derived from a fundamental relationship between the expected number of failure modes surfaced and the cumulative test duration. For convenience, we shall refer to the test duration as test time and measure the reliability as the mean time between system failures (MTBF). The functional form of this fundamental relationship is well known and is easily established without recourse to empiricism (Crow, 1982). We obtain an approximation to this relationship that is suitable for reliability growth planning. One significant advantage to our approach is that it does not rely on an empirically derived relationship such as the Duane based approach. We shall show how the cumulative relationship between the expected number of discovered failure modes and the test time naturally gives rise to a reliability growth relationship between the expected system failure intensity and the cumulative test time. The presented approximation for the resulting growth pattern avoids a number of deficiencies associated with the Duane/MIL-HDBK-189 approach to reliability growth planning.

2.3. Study Overview.

In Section 3 we highlight a number of issues associated with the Duane/MIL-HDBK-189 approach to reliability growth planning. Section 4 develops the exact expected system failure intensity and parsimonious approximations suitable for reliability growth planning. These functions of test time are derived from the exact and planning approximation relationships between the expected number of surfaced failure modes and the cumulative test time. The exact relationship is expressed in terms of the number of potential failure modes, k, and the individual initial failure mode rates of occurrence.

Parsimonious approximations to this relationship are obtained. The first approximation utilizes k and several additional parameters. The second approximation discussed is the limiting form of the first approximation as k increases. This approximation is suitable for complex systems or subsystems. The approximations are derived through consideration of an MTBF projection equation. This equation arises from considering the problem of estimating the system MTBF at the start of a new test phase after implementing corrective actions to failure modes surfaced in a preceding test phase. This MTBF projection has been documented in (Ellner et al., 2004) and is described in Section 4.

Section 5 contains simulation results. The simulations are conducted to obtain actual patterns for the cumulative number of surfaced failure modes versus test time for random draws of initial mode failure rates from several parent populations, and for a geometric sequence of initial mode failure rates. The resulting stochastic realizations are compared to the theoretical expected number of potential surfaced failures modes and to the parsimonious approximations. Random draws for mode fix effectiveness factors (FEFs) (fraction reductions in initial failure mode rates of occurrence due to mitigation) are used to simulate corrective actions to surfaced failure modes. Using the simulated corrective actions, the relationship between the expected system failure intensity and cumulative test time is simulated for various sets of mode initial failure rates. This relationship is obtained under the assumption that the system failure intensity associated with a cumulative test time t reflects implementation of corrective actions to the modes surfaced by t with the associated randomly drawn FEFs. The resulting system MTBF versus test time relationship is compared to the corresponding relationship established for planning purposes.

Section 6 derives expressions for a reliability projection scale parameter that is utilized in the parsimonious approximations. The projection parameter is expressed in terms of basic planning parameters. The resulting MTBF approximations are compared to the reciprocals of the exact expected system failure intensity and stochastic realizations of the system failure intensity, and to MIL-HDBK-189 MTBF approximations based on planning parameters. The comparisons are done for several reliability growth patterns.

Section 7 addresses the relationship between the theoretical upper bound on the achievable system MTBF, termed the growth potential, and the planning parameters. The projection scale parameter considered in Section 6 is then expressed in terms of planning parameters and the MTBF growth potential. It is shown that the scale parameter becomes unrealistically large if the goal MTBF is chosen too close to the growth potential or if the allocated test time to grow from the initial to goal MTBF is inadequate.

Section 8 indicates how to construct a sequence of MTBF target values that start at an expected or measured initial MTBF and end at the goal MTBF. It is shown that the parsimonious approximation to the reciprocal of the expected system failure intensity can be used for this purpose in conjunction with a test schedule that specifies the expected monthly RAM hours to be accumulated on the units under test and the planned corrective action periods.

3. MIL-HDBK-189 IDEALIZED GROWTH CURVE.

3.1. Background.

The frequently referenced United States Department of Defense MIL-HDBK-189 (Department of Defense, 1981) utilizes an idealized reliability growth pattern with failure intensity function $\rho_M(t)$ given by,

$$\rho_M(t) = \lambda_M \beta_M \, t^{\beta_M - 1} \tag{1}$$

Letting $N_M(t)$ denote the number of failures by *t*, the corresponding expected number of failures by *t* is given by,

$$E\big(N_M(t)\big) = \lambda_M \, t^{\beta_M} \tag{2}$$

For planning purposes, the handbook divides the allocated test time *T* into *p* test phases that end at the cumulative test times $t_1 < t_2 < \ldots < t_p = T$. Reliability growth may occur within a test phase. However, the MIL-HDBK-189 approach does not assume the growth pattern governed by Equation (1) holds within each test phase. For example, no corrective actions may be applied within some test phases. The test phases typically are separated by blocks of calendar time during which a significant number of corrective actions are implemented to failure modes surfaced in the preceding test phase. Thus jumps in reliability are typically expected from test phase to test phase. For planning, the handbook only assumes that Equation (2) holds at the ends of the test phases, i.e., for $t = t_i$. In particular, the points with coordinates $\left(t_i, \frac{E(N_M(t_i))}{t_i}\right)$ are assumed to lie on a straight line on a log-log plot of $\frac{E(N_M(t_i))}{t_i}$ versus t_i with slope equal to $-\alpha_M$. The value α_M is called the growth rate. The parameter β_M that appears in Equation (2) is equal to $1-\alpha_M$. The assumption in the handbook is motivated by Duane's empirical relationship (Duane, 1964). Duane observed that, for a number of data sets, the logarithm of the cumulative failure rate versus the logarithm of the cumulative test time tended to display a linear relationship. Note, however, Duane's observations were based on fitting straight lines to test data using a log-log scale and thus presumably applied to the observed pattern of growth during a test phase as opposed to across test phases although this is not addressed in (Duane, 1964). In fact, although for planning purposes MIL-HDBK-189 does not assume Equation (2) holds within all the test phases, the handbook does utilize a power law relationship for estimating reliability in a test phase, i.e., for tracking reliability growth within a test phase. The use of Equation (2) for this purpose seems more tied to Duane's observations.

3.2. Depicting the Planned Reliability Growth.

The MIL-HDBK-189 approach utilizes average MTBF values over each test phase to depict the planned reliability growth path. For test phases during which no corrective actions are expected to be implemented this average MTBF would also be the instantaneous MTBF. The one structured method presented in the handbook to obtain these test phase average MTBF values is based on first specifying an idealized curve that

satisfies Equation (2) at the end of each test phase. The idealized curve is frequently determined by specifying a planned or assessed average MTBF, M_1, over the initial test period, the total test time over all the test phases, *T*, and the goal MTBF, M_G, to be attained at *T*. The growth rate α_M can then be solved for and the constants $\beta_M = 1 - \alpha_M$ and λ_M that appear in Equation (2) can be obtained. For test phase *i*, the average failure rate ϕ_i is defined by,

$$\phi_i = \frac{E(N_M(t_i)) - E(N_M(t_{i-1}))}{t_i - t_{i-1}} \tag{3}$$

The corresponding average MTBF for phase *i* is taken to be the reciprocal of ϕ_i. The pattern of test phase MTBF averages so obtained do not explicitly take into account parameters that can be directly influenced by program management. Such parameters include the management strategy (MS), the average fix effectiveness factor (μ_d), the corrective action lag time, and the scheduled monthly RAM test hours and corrective action periods. If one explicitly takes into account these factors, the growth pattern exhibited by the resulting test phase MTBFs, even when displayed on a test time basis, will often look more irregular than the pattern of average test phase MTBFs obtained from the MIL-HDBK-189 approach. In particular, this growth pattern may not be well represented by a pattern consistent with Equation (1).

The reciprocal of the idealized failure intensity given in (1) is considered to be a representation of the overall MTBF growth trend over the test program after the first test phase. Note for growth one has α_M greater than zero. Thus as *t* approaches zero the MTBF implied by Equation (1) approaches zero. Therefore, for planning purposes, the handbook utilizes Equation (1) to represent the overall growth trend only for $t > t_1$. The handbook simply utilizes a constant or average failure rate, $\phi_1 = M_1^{-1}$, over the first test phase. The constant ϕ_1 is chosen such that Equation (2) is satisfied for $t = t_1$. Doing so, it follows that the MTBF growth trend consistent with Equation (1) for $t > t_1$ and ϕ_1 is given by,

$$MTBF(t) = \begin{cases} M_1 & 0 \le t \le t_1 \\ M_1 \left(\dfrac{t}{t_1}\right)^{\alpha_M} (1-\alpha_M)^{-1} & t > t_1 \end{cases} \tag{4}$$

3.3. MIL-HDBK-189 Planning Model Issues.

In using Equation (4) one must be careful not to automatically equate M_1 to the planning parameter M_I, defined as the initial MTBF. In general, $M_I \le M_1$. The two MTBFs should be equated only if no growth is planned over the first test phase, since M_1 is the planned average MTBF over the initial test phase.

The growth rate α_M is used as a measure of programmatic risk with respect to being able to grow from M_1 to $M_G = MTBF(T)$ in test time *T*. The higher the α_M relative to past experience the greater the risk of attaining M_G. From Equation (4) we can see that $MTBF(T)$ is a strictly increasing function of the ratio T/t_1 and can be made as large as desired by making t_1 sufficiently small. Thus for any given *T*, M_1, and growth rate α_M

one can always find a small enough t_1 such that $MTBF(T)$ will equal the desired value. This implies that α_M as a measure of programmatic risk is only as meaningful as the choice of t_1. In particular, one should guard against artificially lowering α_M by selecting t_1 so small that no significant amount of fix implementation is expected to occur until during a corrective action period that is beyond t_1. The strong dependence of the global parameter α_M on the length of the initial test phase is not a desirable attribute for planning purposes.

Finally, we note that Equation (4) implies that, even with a reasonable choice for t_1, any value of M_G can eventually be obtained since there is no upper limit implied by Equation (4). This is true even using a growth rate that appears to be reasonable based on past experience with similar types of systems. However, one must keep in mind that if the planning curve extends over many thousands of hours, the planned growth rate may not be sustainable due to resource constraints besides test time and due to technological constraints. Past comparable growth rates may have been estimated from test data over one test phase of a much shorter duration and the system may also have been relatively immature.

4. DERIVED RELIABILITY GROWTH PATTERNS.

4.1 Assumptions.

The system has a large number of potential failure modes with initial rates of occurrence $\lambda_1,...,\lambda_k$. The modes are candidates for corrective action if they are surfaced during test. All failure modes independently generate failures according to the exponential distribution and the system fails whenever a failure mode occurs. It is also assumed that corrective actions do not create new failure modes.

4.2 Background Information.

The first step in obtaining a functional form for the expected failure intensity as a function of test time and planning parameters that is based on non-empirical considerations involves the relationship between the expected number of failure modes surfaced and test duration. This relationship was considered by Crow (1982) for the case where test duration is continuous. In this paper we are measuring test duration in a continuous fashion. Test time will be used as a generic measure of test duration for this continuous case. The relationship is easily obtained by expressing the number of surfaced modes by test time *t* as a sum of mode indicator functions. In particular, let $I_i(t)$ denote the indicator function for mode *i*. The indicator function takes on the value one if mode *i* occurs by *t* and equals zero otherwise. The number of modes surfaced by *t* is given by,

$$M(t) = \sum_{i=1}^{k} I_i(t) \tag{5}$$

The expected value of $M(t)$ is equal to,

$$\mu(t) = \sum_{i=1}^{k} E(I_i(t)) = \sum_{i=1}^{k} (1 - e^{-\lambda_i t}) = k - \sum_{i=1}^{k} e^{-\lambda_i t} \tag{6}$$

This expected value function implies a functional form for the expected failure intensity and corresponding MTBF as a function of test time *t* given that corrective actions have been incorporated to all the failure modes surfaced by *t*. One component of the expected failure intensity is due to the failure modes not yet surfaced by *t*. This component is simply given by the derivative of $\mu(t)$. Note,

$$\frac{d\mu(t)}{dt} = \sum_{i=1}^{k} \lambda_i e^{-\lambda_i t} \tag{7}$$

In (Ellner et al., 2000) it is shown that the expression in (7) is the expected failure intensity due to all the modes not surfaced by *t*. To show this observe that the failure intensity due to these modes can be expressed as the random variable $\Lambda_U(t)$ where

$$\Lambda_U(t) = \sum_{i=1}^{k} \lambda_i \left(1 - I_i(t)\right) \tag{8}$$

The expected value of $\Lambda_U(t)$ is given by,

$$E\left(\Lambda_U(t)\right) = \sum_{i=1}^{k} \lambda_i \{1 - E\left(I_i(t)\right)\} = \sum_{i=1}^{k} \lambda_i e^{-\lambda_i t} = \frac{d\mu(t)}{dt} \tag{9}$$

Before considering the other components of the system failure intensity, we shall address obtaining parsimonious approximations to the expected number of failure modes surfaced by t and the corresponding failure intensity due to the unsurfaced failure modes. The exact expressions for these quantities are given by (6) and (9). Note that these expressions depend on k +1 parameters, namely the number of potential failure modes k and the initial failure mode rates of occurrence λ_i for $i = 1,...,k$.

4.3 Parsimonious Approximations.

4.3.1 Expected Number of Modes and its Derivative.

To obtain parsimonious approximations to the expected number of modes surfaced by t and its derivative, we shall consider an optimization problem under the assumption that all corrective actions are delayed until t. Let N_i denote the number of failures that occur by t due to mode i. Then $\hat{\lambda}_i = \frac{N_i}{t}$ denotes the standard Maximum Likelihood Estimate (MLE) of λ_i. Consider the estimator for λ_i given by,

$$\tilde{\lambda}_i = \theta \cdot \hat{\lambda}_i + (1-\theta) \cdot avg(\hat{\lambda}_i) \tag{10}$$

where $avg(\hat{\lambda}_i)$ denotes the arithmetic average of the k $\hat{\lambda}_i$ and $\theta \in [0,1]$ is chosen to minimize the expected sum of squared errors between $\tilde{\lambda}_i$ and λ_i, i.e. $E\left[\sum_{i=1}^{k}(\tilde{\lambda}_i - \lambda_i)^2\right]$. The value of θ that solves this optimization problem can be shown to be θ_S (Ellner et al., 2004) where

$$\theta_S = \frac{Var[\lambda_i]}{\frac{\lambda}{k \cdot t}\left(1 - \frac{1}{k}\right) + Var[\lambda_i]} \tag{11}$$

for $\lambda = \sum_{i=1}^{k} \lambda_i$, $\bar{\lambda} = \frac{\lambda}{k}$, and $Var[\lambda_i] = \frac{\sum_{i=1}^{k}(\lambda_i - \bar{\lambda})^2}{k}$. The estimate of λ_i given by (10) with θ equal to θ_S has been called the Stein estimate of λ_i (Ellner et al., 2004). Note this is a theoretical estimate in the sense that it cannot be computed from the data since it involves the unknown values of k, λ, and $Var[\lambda_i]$. The quantity $Var[\lambda_i]$ can also be expressed as follows:

$$Var[\lambda_i] = \left(\frac{1}{k}\right)\left(\sum_{i=1}^{k} \lambda_i^2 - \frac{\lambda^2}{k}\right) \tag{12}$$

From the definition of $\tilde{\lambda}_i$ and the fact that N_i equals zero for a failure mode unobserved by t we have that the Stein assessment for the failure rate contribution of a failure mode not observed by t is given by,

$$\tilde{\lambda}_i = (1-\theta_S) \cdot \left(\frac{N}{k \cdot t}\right) \tag{13}$$

Thus the Stein assessment of the failure intensity due to all the failure modes not surfaced by t equals,

$$\sum_{i\in\overline{obs}} \tilde{\lambda}_i = (k-m)\cdot(1-\theta_S)\cdot\left(\frac{N}{k\cdot t}\right) = \left(1-\frac{m}{k}\right)\cdot(1-\theta_S)\cdot\left(\frac{N}{t}\right) \tag{14}$$

where m denotes the number of surfaced modes by t and $\overline{obs}$ denotes the index set for the failure modes not surfaced by t. From (11) and (12) one can show,

$$1-\theta_S = \frac{\left(\frac{\lambda}{k\cdot t}\right)\cdot\left(1-\frac{1}{k}\right)}{\left(\frac{1}{k}\right)\cdot\left(\sum_{i=1}^{k}\lambda_i^2 - \frac{\lambda^2}{k}\right) + \left(\frac{\lambda}{k\cdot t}\right)\cdot\left(1-\frac{1}{k}\right)} \tag{15}$$

Replacing $1-\theta_S$ in (14) by the final expression in (15) and simplifying yields,

$$\sum_{i\in\overline{obs}} \tilde{\lambda}_i = \frac{\left(1-\frac{1}{k}\right)\cdot\left(1-\frac{m}{k}\right)\cdot\left(\frac{N}{t}\right)}{\left(1-\frac{1}{k}\right) + \left(\frac{\sum_{i=1}^{k}\lambda_i^2}{\lambda} - \frac{\lambda}{k}\right)\cdot t} \tag{16}$$

Equation (16) gives the Stein assessment for the failure intensity due to all the failure modes not surfaced by t. Note that m can be regarded as an estimate of the expected number of modes surfaced by t, i.e. $\mu(t)$. Additionally, in light of Equation (9), the left hand side of (16) can be viewed as an estimate of $\frac{d\mu(t)}{dt}$. From (7), it follows that the derivative of $\mu(t)$ at $t=0$ equals λ. Finally, observe that $\frac{N}{t}$ in (16) is the maximum likelihood estimate of the initial failure rate λ under the assumption that all corrective actions are delayed to t. Let $h(t)$ denote $\frac{d\mu(t)}{dt}$. Simulation results for a number of cases (where k and the λ_i are known) conducted in support of (Ellner et al., 2004) have indicated that the Stein assessment given in (16) yields good estimates of $h(t)$ when all the corrective actions are delayed. The value $h(t)$ that is being estimated does not depend on the corrective action process. Only the estimate of λ given by $\frac{N}{t}$ depends on the assumption that all corrective actions are delayed until t. Thus the right hand side of (16) with m and $\frac{N}{t}$ replaced by good approximations of $\mu(t)$ and $\lambda = \left.\frac{d\mu(t)}{dt}\right|_{t=0}$ respectively should yield a good approximation for $h(t)$ irregardless of the corrective action process for the cases where the Stein estimate of $h(t)$ given by (16) are accurate. This suggests that we choose our parsimonious approximation for $\mu(t)$, denoted by $\mu_k(t)$, as the unique solution to the differential equation obtained from (16) by replacing m by $\mu_k(t)$, $\frac{N}{t}$ by λ, and $\sum_{i\in\overline{obs}} \tilde{\lambda}_i$ by $\frac{d\mu_k(t)}{dt}$ with initial conditions $\mu_k(0)=0$ and $\left.\frac{d\mu_k(t)}{dt}\right|_{t=0} = \lambda$. For the case where all the λ_i are equal, one can show that $\mu_k(t) = \mu(t)$ for all $t \geq 0$. Thus, in what follows we shall only consider the case where not all the λ_i are equal. The solution to the resulting differential equation, for this case, with the specified initial conditions is,

$$\mu_k(t) = k \cdot \left[1 - \left(1 + \beta_k \cdot t\right)^{-p_k}\right] \tag{17}$$

where

$$\beta_k = \left(1 - \frac{1}{k}\right)^{-1} \left[\left(\frac{1}{\lambda}\right)\left(\sum_{i=1}^{k} \lambda_i^2\right) - \frac{\lambda}{k}\right] \tag{18}$$

and

$$p_k = \frac{\lambda}{k \cdot \beta_k} \tag{19}$$

The solution was obtained by the method of integrating factors (Boyce et al., 1965). The solution can be verified by directly substituting (17) and its derivative into the differential equation for $\mu_k(t)$ and noting that $\mu_k(t)$ satisfies the specified initial conditions. Observe that $\mu_k(t)$ can be expressed in terms of *t* and three constants, namely *k*, λ and β_k. The corresponding parsimonious approximation for $h(t)$ is $\frac{d\mu_k(t)}{dt}$, which we shall denote by $h_k(t)$.

It is interesting to note that $\mu_k(t)$ given by (17) is the same expression that one can obtain for the expected number of software bugs surfaced in execution time *t* given by the doubly stochastic exponential order model presented in (Miller, 1985) for the case where the initial bug occurrence rates $\lambda_1, \ldots, \lambda_k$ constitute a realization of a random sample of size *k* from a gamma random variable. The density function of this random variable is given by,

$$f(x) = \begin{cases} \dfrac{x^{\alpha_k} \cdot e^{-\left(\frac{x}{\beta_k}\right)}}{\Gamma\left(\alpha_k + 1\right) \cdot \beta_k^{(\alpha_k + 1)}} & \text{for } x > 0 \\ 0 & \text{otherwise} \end{cases}$$

In this density function, Γ denotes the gamma function, β_k is defined by (18), and $\alpha_k + 1$ equals p_k. This result is shown in (Ellner et. al., 2000) where $\mu_k(t)$ denotes the expected number of surfaced modes by time *t* that will be mitigated by a corrective action.

4.3.2 Expected System Failure Intensity and MTBF.

Next we shall consider the expected system failure intensity after *t* test hours and a corresponding parsimonious approximation, given that corrective actions are implemented to all the surfaced failure modes. We shall let d_i denote the fraction reduction in the rate of occurrence of mode *i* due to the corrective action (termed a fix). The reduction factor is termed the fix effectiveness factor (FEF) for failure mode *i*. Let $\Lambda(t)$ denote the failure intensity of the system given that fixes have been incorporated to all the failure modes surfaced by *t*. Then,

$$\Lambda(t) = \sum_{i=1}^{k} \left(1 - d_i I_i(t)\right)\lambda_i \tag{20}$$

The corresponding expected failure intensity is $\rho(t)$ where,

$$\rho(t) = E\left(\Lambda(t)\right) = \sum_{i=1}^{k} \left(1 - d_i E\left(I_i(t)\right)\right)\lambda_i = \sum_{i=1}^{k} \left(1 - d_i\right)\lambda_i + \sum_{i=1}^{k} d_i \lambda_i e^{-\lambda_i t} \tag{21}$$

This expression for the expected failure intensity was presented in (Crow, 1982).

For reliability growth planning purposes, assessments of individual failure mode FEFs will not be available. Thus, in place of $\rho(t)$ we shall use a parsimonious approximation, denoted by $\rho_k(t)$, that utilizes an average fix effectiveness factor. It follows from (9) that $\lambda - h(t)$ is the expected failure intensity due to the failure modes surfaced by *t* prior to mitigation. Assume these modes are mitigated with an average FEF of μ_d. Then the expected failure intensity due to the surfaced failure modes after mitigation can be approximated by $(1-\mu_d)\cdot(\lambda - h(t))$. Thus the parsimonious approximation for $\rho(t)$ will be defined as follows:

$$\rho_k(t) = (1-\mu_d)\cdot(\lambda - h_k(t)) + h_k(t) \tag{22}$$

We also define the parsimonious MTBF approximation of $MTBF(t) = (\rho(t))^{-1}$ for reliability growth planning by $MTBF_k(t) = (\rho_k(t))^{-1}$.

For planning, it can be useful to add a term, λ_A, to the expressions for $\rho(t)$ and $\rho_k(t)$ given by (21) and (22) respectively. This term represents the failure rate due to all the failure modes that will not be corrected, even if surfaced … referred to as A-modes (Crow, 1982). This term for planning purposes would be given by the quantity $(1-MS)\cdot\lambda$. However, since this term does not contribute to the difference between $\rho(t)$ and $\rho_k(t)$ we shall not consider it further in this section or Section 5.

It may be difficult to select a value of *k* for planning purposes. For complex systems or subsystems it is reasonable to use the limiting forms of $\mu_k(t)$, $h_k(t)$, and $\rho_k(t)$ as $k \to \infty$. Consider the limit as $k \to \infty$ of these functions. In taking the limit we shall hold λ fixed and assume the limit of β_k is positive as *k* increases, say $\beta_\infty \in (0,\infty)$. Under these conditions one can show the three functions converge to limiting functions which we shall denote by $\mu_\infty(t)$, $h_\infty(t)$, and $\rho_\infty(t)$, respectfully. One can show,

$$\mu_\infty(t) = \left(\frac{\lambda}{\beta_\infty}\right)\ln(1+\beta_\infty \cdot t) \tag{23}$$

and

$$h_\infty(t) = \frac{d\mu_\infty(t)}{dt} = \lambda(1+\beta_\infty \cdot t)^{-1} \tag{24}$$

Also, $\rho_\infty(t)$ is given by (22) with $h_k(t)$ replaced by $h_\infty(t)$.

5. SIMULATION.

5.1 Simulation Overview.

We wish to compare the parsimonious approximations to realized and expected reliability growth patterns with respect to a number of quantities. To do so we shall generate a number of realized reliability growth patterns via simulation in Mathematica. We shall consider cases where the failure mode initial rates of occurrence are realizations of a specified parent population for several choices of the parent distribution. We shall also generate reliability growth patterns for a deterministically specified sequence of failure mode initial rates of occurrence that have been found to be useful in representing initial bug rates of occurrence in software programs under development (Miller, 1985). The simulation consists of the following steps:

(1) Specify inputs. This includes items such as, 1. test duration, 2. the number of failure modes, and 3. the sequence or parent population governing the initial mode failure rates.
(2) Produce mode initial failure rates. Failure rates are either stochastically generated, or deterministically calculated. In the stochastic case, failure rates are generated by drawing realizations of a random sample from a specified gamma, Weibull, lognormal or loglogistic (Meeker et al., 1998) parent population. In the deterministic case, failure rates are calculated in accordance with a specified geometric sequence.
(3) Generate mode failure times. The mode failure times are generated via a function of randomly generated uniform numbers, and the mode initial failure rates.
(4) Generate mode fix effectiveness factors. The FEFs are generated by drawing realizations of a random sample from a beta distribution with mean 0.80, and coefficient of variation 0.10.
(5) Examine quantities and plots of interest.

5.2 Simulation Results.

Results below display plots of the expected and realized number of surfaced failure modes for stochastic λ_i generated from a loglogistic (Figure 1), and deterministic λ_i calculated from a geometric sequence (Figure 3). Also shown are plots of the reciprocals (i.e. MTBFs) of the expected and realized system failure intensities for loglogistic λ_i (Figure 2), and geometric λ_i (Figure 4). The geometric initial mode failure rates are given by

$$\lambda_i = a \cdot b^i \tag{25}$$

for $i = 1,\ldots,k$ where $0 < a$ and $0 < b < 1$. All the displayed quantities have been averaged over ten replications of simulation steps (2) through (4) above.

The intent of the plots is to see whether the functional form of the parsimonious approximations are reasonably compatible with respect to (1) the expected number of surfaced failure modes as a function of test time, and (2) the reciprocal of the expected system failure intensity as a function of test time. Corrective actions are assumed to be implemented to all the failure modes surfaced by t with the simulated mode fix

effectiveness factors. The value of μ_d in Equation (22) is set equal to $\frac{1}{k}\sum_{i=1}^{k} d_i$ to generate the parsimonious approximations to the exact expected failure intensity and corresponding MTBF. Additionally, for the results displayed below, $k = 1{,}500$ and $\lambda = 10^{-1}$.

The value of the scale parameter obtained from Equation (18) does not provide adequate parsimonious approximations except when the parent population is gamma or the scale parameter is sufficiently small. Thus for the specified *k*, μ_d, and λ, the scale parameters β_k and β_∞ of the parsimonious approximations were fitted to the exact expected number of surfaced failure modes function by using maximum likelihood estimates. These estimates were obtained from the simulated mode first occurrence times. This was accomplished by assuming the generated initial mode failure rates $\lambda_1, \ldots, \lambda_k$ represented a realization of a random sample of size *k* from a gamma distribution with scale parameter β_k and mean λ/k. This procedure provided a "best statistical fit" of the parsimonious functional approximations for $\mu(t)$ and $\rho(t)$, with respect to the scale parameter, over the entire planning period of interest, i.e. 10,000 hours.

The parsimonious approximations for $\mu(t)$ and $\rho(t)$ based on the limiting forms for $\mu_k(t)$ and $\rho_k(t)$ as *k* increases will tend to be too large for values of *t* when $\mu(t)$ is too close to *k*. We have observed that the limiting approximations are adequate for $\mu(t)$ and $\rho(t)$ over the range of *t* for which $\mu(t) \le k/5$. Thus for complex systems, or subsystems, the limiting approximation functional forms should be adequate representations of $\mu(t)$ and $\rho(t)$ over most test periods of interest.

The red curves in the figures below represent the exact expected number of surfaced modes (Figures 1, and 3), or the reciprocal of the exact expected system failure intensity (Figures 2 and 4). The dots in each figure represent a corresponding stochastic realization. The green curves display the finite *k* approximations while the blue curves display the corresponding limiting approximations. The displayed curves and stochastic realizations are averages over ten replications of simulation steps (2) through (4). Similar results were obtained for the cases where the λ_i were generated from gamma, lognormal, and Weibull parent populations.

For comparison purposes, the MIL-HDBK-189 system MTBF based on Equation (4) was fitted to the reciprocal of the expected system failure intensity (the red curves). The MIL-HDBK-189 curves are displayed in yellow and were fitted utilizing all the observed simulated cumulative times of failure. The use of all cumulative failure times requires that fixes be implemented when failure modes are observed. The simulation was carried out in this manner to allow the parameters of the MIL-HDBK-189 curves to be statistically fitted via the maximum likelihood estimation procedure in (Department of Defense, 1981). As for the other displayed quantities, the averages of 10 replicated MIL-HDBK-189 MTBF curves are shown.

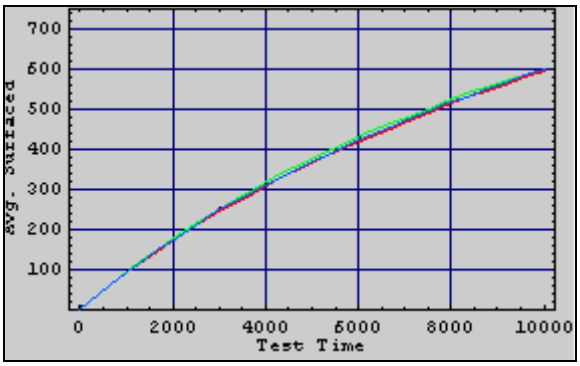

Figure 1. Avg. No. Surfaced Modes (Loglogistic).

Notice the high degree of accuracy displayed in Figure 1 for the finite and infinite *k* approximations despite violating the gamma assumption used to statistically fit the parsimonious approximations.

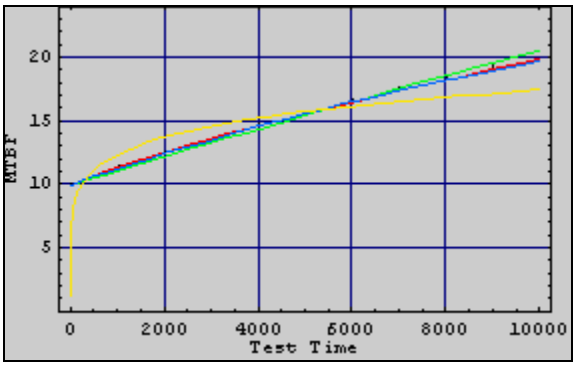

Figure 2. Reciprocal of the Failure Intensity (Loglogistic).

Figure 2 displays a high degree of accuracy for the statistically fitted PM2 MTBF approximations despite violating the MLE assumption that the initial mode failure rates are gamma distributed. In addition, the PM2 approximations of the MTBF appear favorable to that of the MIL-HDBK-189 model.

Figure 3 and 4 below are analogous to Figures 1 and 2, respectively. The only difference is the generation procedure associated with the initial mode failure rates utilized in the analysis. In this case, failure rates are deterministically calculated in accordance with a geometric sequence. The results are similar.

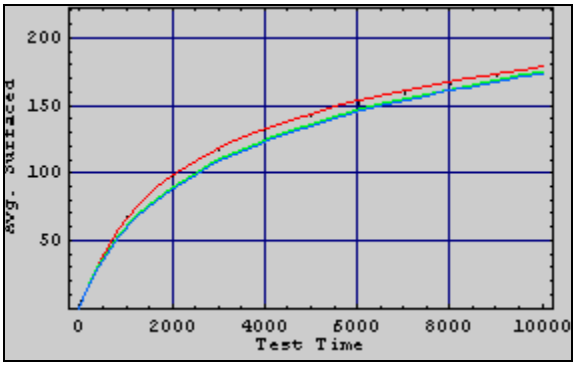

Figure 3. Avg. No. Surfaced Modes (Geometric).

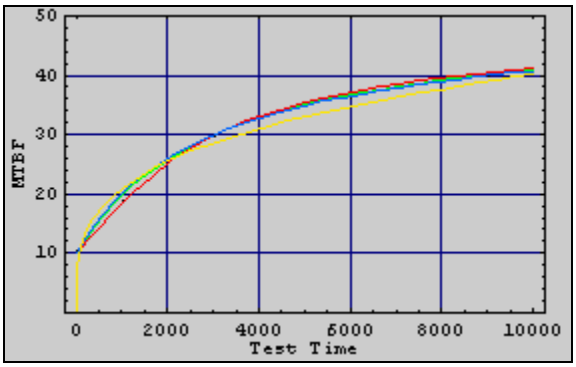

Figure 4. Reciprocal of the Failure Intensity (Geometric).

6. USING PLANNING PARAMETERS TO CONSTRUCT THE PARSIMONIOUS MTBF GROWTH CURVE.

6.1 Methodology.

6.1.1 Planning Formulae not Using Failure Mode Classification.

In the previous sections, a functional form for the planned MTBF growth curve was developed. It was indicated that this functional form was compatible with a number of potential growth patterns. In Section 5 the simulation produced failure mode first occurrence times from a set of initial mode failure rates. For each simulation replication, the parsimonious MTBF growth pattern was derived from a statistically fitted parsimonious expression for the expected number of failure modes function. This was accomplished by utilizing the mode first occurrence times to obtain a MLE of scale parameter β subject to the initial failure intensity λ held fixed to a specified value (e.g. λ = 0.10 in Section 5). In practice, the initial mode rates of occurrence will not be available to obtain the planning curve parameter β.

In this section we shall develop formulas for β in terms of the planning parameters T, M_I, M_G, and average FEF μ_d (and k for the finite case). We shall also address the question of how well the parsimonious MTBF planning curves based on the resulting values of β captures several potential reliability growth patterns that depend on realized values of $\lambda_1,\ldots,\lambda_k$ and $d_1,\ldots,d_k$.

As indicated in Section 4, the form of the parsimonious expected system failure intensity is,

$$\rho_{PL}(t) = (1-\mu_d)(\lambda - h(t)) + h(t) \tag{26}$$

For complex systems,

$$h(t) = \frac{\lambda}{1+\beta\cdot t} \tag{27}$$

where $0 \le t \le T$. For the finite k case, the equation for $\rho_{PL}(t)$ remains the same with $h(t)$ replaced by $h_k(t) = \frac{\lambda}{(1+\beta_k\cdot t)^{p_k+1}}$ where $p_k = \lambda / k\cdot\beta_k$ and β_k denotes the planning value of β for finite k.

To develop formulas for β in terms of planning parameters, let $\theta(t)$ denote the expected fraction of λ attributed to the failure modes surfaced by t. Thus,

$$\theta(t) = \frac{\lambda - h(t)}{\lambda} = 1 - \frac{h(t)}{\lambda} \tag{28}$$

This yields,

$$h(t) = \lambda\cdot(1-\theta(t)) \tag{29}$$

It follows that,

$$\rho_{PL}(t) = (1-\mu_d)\{\lambda\cdot\theta(t)\} + \lambda\cdot\{1-\theta(t)\} = \{1-\mu_d\cdot\theta(t)\}\cdot\lambda \tag{30}$$

Let M_G denote the goal MTBF at $t = T$ and $\lambda_G = M_G^{-1}$. Then we set

$$\lambda_G = \rho_{PL}(T) = \{1-\mu_d\cdot\theta(T)\}\cdot\lambda \tag{31}$$

Thus,

$$\theta(T)=\left(\frac{1}{\mu_d}\right)\left(1-\frac{M_I}{M_G}\right) \tag{32}$$

For finite k let $\theta(t)=\theta_k(t)$ where $\theta_k(t)=1-\frac{h_k(t)}{\lambda}=1-(1+\beta_k\cdot t)^{-(p_k+1)}$. In the above β_k is the solution to the equation (32) with $\theta(T)=\theta_k(T)$ where $p_k = \lambda/k\cdot\beta_k$.

Note for the complex system case,

$$\theta(t)=1-\frac{h(t)}{\lambda}=\frac{\beta\cdot t}{1+\beta\cdot t} \tag{33}$$

Therefore, for this case

$$\frac{\beta\cdot T}{1+\beta\cdot T}=\left(\frac{1}{\mu_d}\right)\left(1-\frac{M_I}{M_G}\right) \tag{34}$$

Solving for β yields,

$$\beta=\left(\frac{1}{T}\right)\left(\frac{1-\frac{M_I}{M_G}}{\mu_d-\left(1-\frac{M_I}{M_G}\right)}\right) \tag{35}$$

6.1.2 Planning Formulae Using Failure Mode Classifications.

In some cases the set of failure modes can be split into two categories termed A-modes and B-modes (Crow, 1982). The B-modes are failure modes that will be mitigated if surfaced during test. The A-modes are those that will not receive a corrective action even if observed during test. For this case, the parsimonious expected failure intensity would be,

$$\rho_{PL}(t)=\lambda_A+(1-\mu'_d)(\lambda_B-h_B(t))+h_B(t) \tag{36}$$

where λ_A is the failure intensity due to A-modes, λ_B is the initial failure intensity due to B-modes (thus $\lambda=\lambda_A+\lambda_B$), $h_B(t)$ is the expected failure intensity due to the set of B-modes not surfaced by *t*, and μ'_d is the average FEF that would be realized for the B-modes if all were surfaced during test. For complex systems, $h_B(t)$ is given by $\frac{\lambda_B}{1+\beta\cdot t}$. Using an argument similar to the one in Section 6.1.1 it can be shown that for this case planning formula (35) becomes,

$$\beta=\left(\frac{1}{T}\right)\left(\frac{1-\frac{M_I}{M_G}}{MS\cdot\mu'_d-\left(1-\frac{M_I}{M_G}\right)}\right) \tag{37}$$

where $MS=\lambda_B/\lambda$. The planning parameter *MS* is termed the management strategy. This represents the fraction of λ that is due to the initial B-mode failure intensity. For the finite k case, $h_B(t)$ is given by $\frac{\lambda_B}{(1+\beta_k\cdot t)^{p'_k+1}}$ where $p'_k=\frac{\lambda_B}{k\cdot\beta_k}$. The value β_k solves

Equation (32) with $\theta(T)$ replaced by $\theta_{k,B}(T) = 1 - (1 + \beta_k \cdot T)^{-(p'_k+1)}$ and μ_d replaced by $MS \cdot \mu'_d$.

6.2 Comparisons of MTBF Approximations Using Planning Parameters.

In what follows, we shall not use failure mode categories. Unlike the planned MTBF growth curve, $MTBF_{PL}(t) = \rho_{PL}^{-1}(t)$, the average MTBF growth path generated from the simulation replications depends on the particular parent population of the λ_i or deterministic formula used to generate the λ_i, together with the generated mode FEFs drawn from a beta distribution. Thus, this average MTBF growth path over $t \in [0, T]$ depends on far more than just *k*, *T*, M_I, M_G, and μ_d. Hence one cannot expect that the planned growth path from M_I to M_G, based solely on the planning parameters, will always closely match the averaged reciprocals of the exact expected system failure intensity. However, as indicated in the preceding sections, the functional form of the parsimonious MTBF planning curve is more compatible with respect to the realized MTBF growth pattern than the MIL-HDBK-189 power law MTBF growth pattern. Additionally, the planning parameters are easier to interpret and directly influence than those utilized in the MIL-HDBK-189 approach.

In a number of instances of practical interest the parsimonious MTBF model based on the planning parameters closely approximates the averaged exact MTBF growth patterns. To consider this, we shall compare the parsimonious MTBF planning curve to the reciprocals of the realized stochastic system failure intensity and expected system failure intensity. For a given simulation replication we shall stochastically generate from a given parent population or deterministically calculate $\lambda_1, \ldots, \lambda_k$, together with corresponding mode FEFs $d_1, \ldots, d_k$. The FEFs are generated on each replication from a beta distribution with a mean of 0.80 and coefficient of variation of 0.10.

To calculate the planning value of β on each simulation replication, we shall set $M_I = \lambda^{-1}$ where $\lambda = \sum_{i=1}^{k} \lambda_i$ and choose $\mu_d = \frac{1}{k}\sum_{i=1}^{k} d_i$ (one could alternately choose μ_d to be the expected value of the beta distribution). The value of M_G is set equal to the reciprocal of the realized value of the stochastic system failure intensity at $t = T$. Then Equation (32) with the appropriate form of $\theta(t)$ is used to obtain the planning β for the finite *k* and complex system cases. The corresponding finite *k* and complex system MTBF planning curves for the replication are given by $MTBF_{PL}(t) = \rho_{PL}^{-1}(t)$ where $\rho_{PL}(t)$ is specified in Equation (26).

The plots below in Figures 5, 6, 8, and 10 compare the average of ten replicated MTBF finite and infinite *k* planning curves (green and blue curves, respectively) to the corresponding averages of the reciprocals of the following failure intensities: (1) stochastic realizations of the system failure intensity (black dots); (2) the expected system failure intensity (red curves) and; (3) MIL-HDBK-189 planning curve failure intensities (yellow curves). For our examples the test period is $T = 10{,}000$ hours and $k = 1{,}500$.

One problem encountered in utilizing planning parameters to generate the MIL-HDBK-189 curves is that, as noted in Section 3, these curves employ an average MTBF

over a selected initial test phase (since the curves interpolate back to a zero MTBF at t = 0). To generate a MIL-HDBK-189 planning curve on each simulation replication using M_I, M_G, and T we have used the initial system MTBF metric given in (Crow, 2004) for power law growth curves. The expression for M_I given in (Crow, 2004), denoted by $M_{I,CE}$, is given by

$$M_{I,CE} = \frac{\Gamma\left(1+\frac{1}{\beta_M}\right)}{\left(\lambda_M\right)^{1/\beta_M}} \tag{38}$$

where λ_M and β_M are the MIL-HDBK-189 power law parameters utilized in Equations (1) and (2). The rationale for the M_I metric given by (38) is not discussed in (Crow, 2004). However, it may have been motivated by the following fact: for a non-homogeneous Poisson process of the number of failures experienced by test time t with mean value function $\lambda_M \cdot t^{\beta_M}$, the time to first failure is Weibull distributed. Moreover, the mean of this Weibull random variable is equal to the right-hand side of Equation (38).

Averages of ten replicated power law MTBF approximations shown in yellow in the figures below were obtained using the M_I metric presented in (Crow, 2004) as follows:

1. Set $M_I = \lambda^{-1}$ where $\lambda = \sum_{i=1}^{k} \lambda_i$ and $\lambda_1, \ldots, \lambda_k$ are the realized failure mode initial rates of occurrence for the replication;
2. On each simulation replication of the realized stochastic system failure intensity, set M_G equal to the reciprocal of the realized failure intensity at t = T;
3. Set $M_I = M_{I,CE}$ and $M_G = \left\{\lambda_M \cdot \beta_M \cdot T^{\beta_M - 1}\right\}^{-1}$. Solve for λ_M and β_M, and;
4. Set $MTBF(t) = \left\{\rho_M(t)\right\}^{-1}$ for $0 \le t \le T$ where $\rho_M(t) = \lambda_M \cdot \beta_M \cdot t^{\beta_M - 1}$. The values for λ_M and β_M that satisfy the two equations in step 3 can readily be shown to satisfy the equations $M_I = \dfrac{T\left\{\Gamma\left(1+\frac{1}{\beta_M}\right)\right\}}{\left(\frac{T}{\beta_M \cdot M_G}\right)^{\frac{1}{\beta_M}}}$, and $\lambda_M = \dfrac{T^{1-\beta_M}}{\beta_M \cdot M_G}$.

First we consider several cases where the λ_i are considered a realization of a random sample of size k from a specified parent population. The reference (Miller, 1985) considers a class of software reliability models where the initial bug rates of occurrence are assumed to represent such realizations.

6.2.1 Gamma Parent Population.

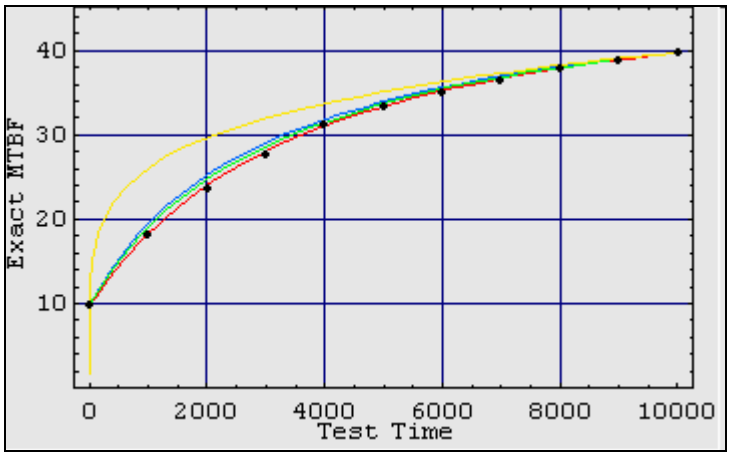

Figure 5. Reciprocal of the Failure Intensity (Gamma).

In Figure 5 above the parent population is a gamma distribution. This distribution has been utilized as a parent population for initial bug rates of occurrence in the software reliability literature (Fakhre-Zakeri et. al., 1992). For this case the averages of the MTBF planning curves for the finite and infinite cases are quite close to the averages of the reciprocals of the realized stochastic and expected system failure intensities. The close approximation is a consequence of the relation mentioned in Section 4 between the solution of the differential equation that defines the parsimonious function $\mu_k(t)$ for the expected number of failure modes surfaced by t and the gamma distribution.

6.2.2 Lognormal Parent Population.

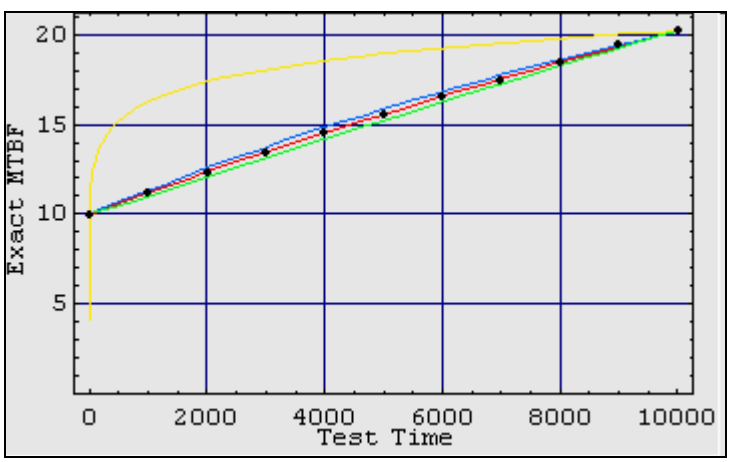

Figure 6. Reciprocal of the Failure Intensity (Log Normal).

In Figure 6 above a lognormal parent population is utilized. For this population, the averaged parsimonious MTBF approximations based on the finite and infinite planning values of β are again close to the averages of the reciprocals of the realized stochastic and expected system failure intensities. However, this close agreement does not always occur, as illustrated in Figure 8. To consider this further, we shall look at the portion of the initial failure intensity that the top w failure modes comprise as a function of w. The top w failure modes refer to a set of failure modes of size w whose initial

failure rates are at least as large as the initial failure rates of the remaining *k-w* modes. More formally, for $i = 1, \ldots, k$ let $\lambda_{(i)}$ denote the ordered mode initial failure rates such that $\lambda_{(1)} \geq \cdots \geq \lambda_{(k)}$. Also let $\eta(w) \equiv \left(\frac{1}{\lambda}\right)\sum_{i=1}^{w} \lambda_{(i)}$ for $w = 1, \ldots, k$ where $\lambda = \sum_{i=1}^{k} \lambda_i$.

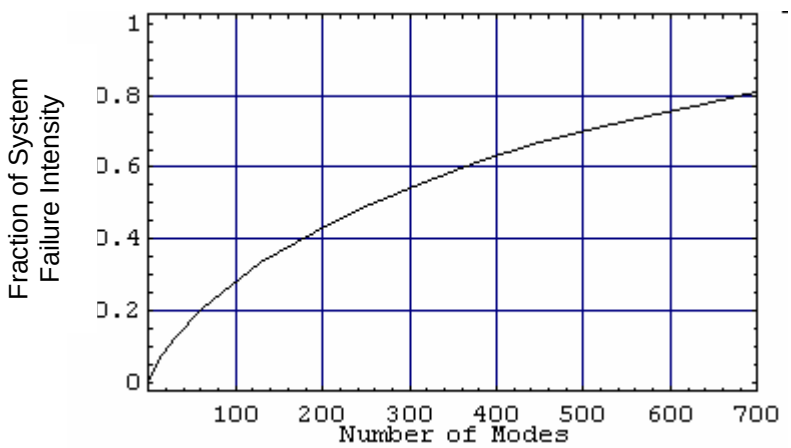

Figure 7. Top W Modes (Log Normal).

The graphs of the average, $\overline{\eta}(w)$, of the ten replicated functions $\eta(w)$ is displayed in Figure 7 for the case where on each replication, $\lambda_1, \ldots, \lambda_k$ was drawn from a lognormal distribution with mean $0.10/k$. This lognormal distribution was also used to generate the ten replicated graphs of the realized and expected system failure intensities on which Figure 6 is based. Note in Figure 7 that $\overline{\eta}(100)$ is less than 0.40.

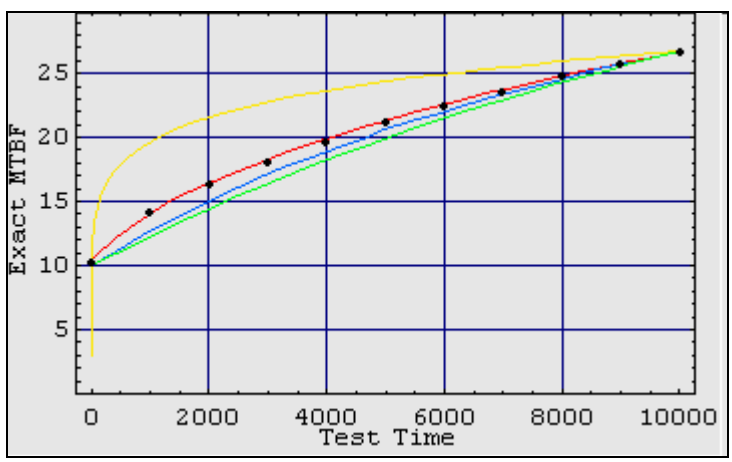

Figure 8. Reciprocal of the Failure Intensity (Log Normal).

Figure 9 is the corresponding graph of $\overline{\eta}(w)$ versus w for the MTBF average curves displayed in Figure 8. The ten replicated system failure intensity curves utilized in Figure 8 are based on the same ten sets of initial mode failure rates used to construct the graph in Figure 9. As for Figures 6 and 7, the lognormal parent population used had a

mean equal to $0.10/k$. However the variance was larger than that of the lognormal utilized for Figures 6 and 7. This resulted in $\overline{\eta}(100) > 0.50$.

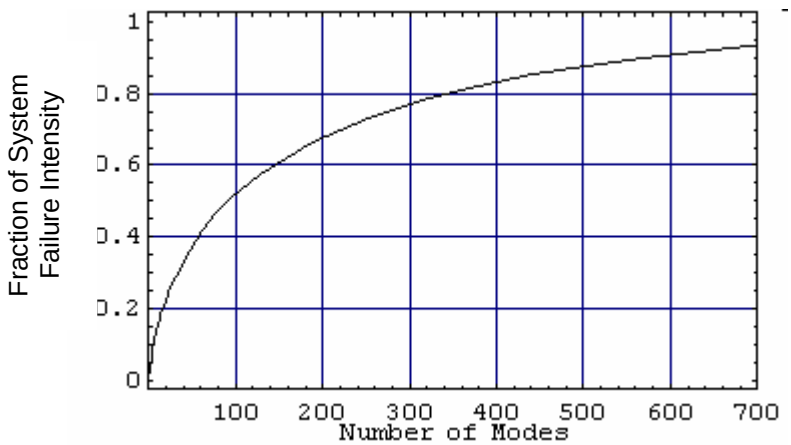

Figure 9. Top W Modes (Log Normal).

In general, the closer the graph of $\overline{\eta}(w)$ is to the line through the origin with slope equal to $1/k$, the closer the averaged MTBF planning curve will be to the averaged reciprocals of the realized stochastic and expected system failure intensities. This follows from the fact that the solution to the differential equation, $\mu_k(t)$, converges to $\mu(t)$ as $\lambda_1,\ldots,\lambda_k$ approach a common value $\lambda_0 > 0$. For the case where $\lambda_i = \lambda_0$ for $i = 1,\ldots,k$ on each replication, the graph of $\overline{\eta}(w)$ versus w for $w = 1,\ldots,k$ lies on the line through the origin with slope equal to $1/k$. Note the graph of $\overline{\eta}(w)$ in Figure 7, although not close to the line through the origin with slope $1/k$, is closer to this line than is the graph of $\overline{\eta}(w)$ displayed in Figure 9. This is consistent with the planning approximation in Figure 6 being more accurate than in Figure 8. The lognormal distribution for the λ_i on which Figures 8 and 9 are based would not be a realistic candidate in many instances for the parent population.

6.2.3 Geometric Initial Mode Failure Rates.

Finally, we consider geometric failure rates, a case where the initial mode failure rates are specified deterministically. For this case recall $\lambda_i = a \cdot b^i$ for $i = 1,\ldots,k$ where $a > 0$ and $0 < b < 1$. According to Miller (1985), such bug initial failure rates have been estimated during replicated – run software debugging experiments (Nagel, 1984, 1982). For such a deterministic case, only the set of associated FEFs $d_1,\ldots,d_k$ are regenerated from the beta distribution on each replication. Note that one can show,

$$\lambda = \sum_{i=1}^{k} \lambda_i = a \cdot \sum_{i=1}^{k} b^i = a \cdot b \cdot \left(\frac{1-b^k}{1-b} \right) \tag{39}$$

Thus,

$$M_I = \left(\frac{1-b}{a \cdot b} \right) \left(1 - b^k \right)^{-1} \tag{40}$$

Also, as before on each simulation replication, λ_G is set equal to the realized value of the stochastic system failure intensity at $t = T$ and $M_G = \lambda_G^{-1}$. To calculate the MTBF planning curve on the replication, in addition to T, M_I, and M_G, the average FEF value μ_d must be specified. We set $\mu_d = \frac{1}{k}\sum_{i=1}^{k} d_i$ (an alternate possibility would be to set μ_d equal to the specified mean of the beta distribution). Figure 10 displays the averages of the ten MTBF planning curves for the finite and infinite cases over the replications (green and blue curves, respectively). These average curves are compared to the averaged reciprocals of the realized stochastic system failure intensities (black dots) and the expected system failure intensities (red curve). Also displayed, is the average of the ten MIL-HDBK-189 planning curves (yellow curve). These are based on T, M_G, and $M_I = M_{I,CE}$.

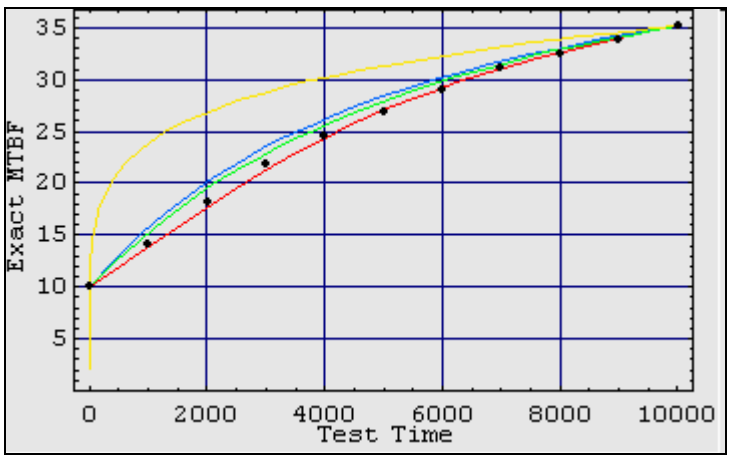

Figure 10. Reciprocal of the Failure Intensity (Geometric).

Figure 11 displays the graph of $\overline{\eta}(w) = \eta(w)$ versus w.

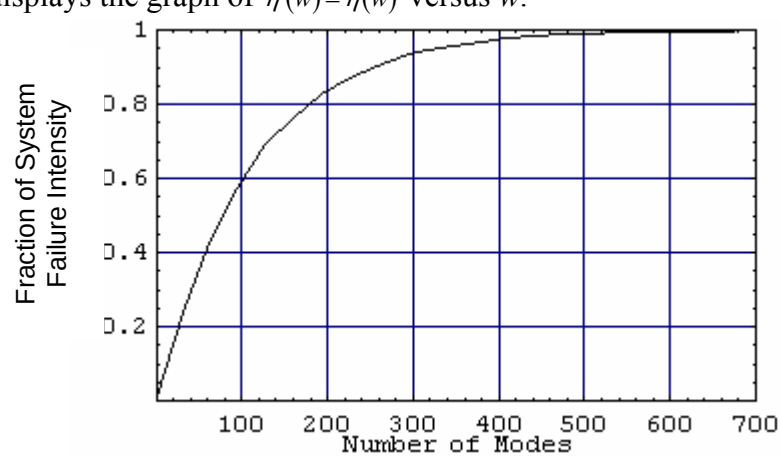

Figure 11. Top W Modes (Geometric).

Even though the top 100 modes account for 60% of the initial failure intensity, the finite and infinite averages of the 10 replicated PM2 planning curves are reasonably compatible with the averages of the reciprocals of the 10 corresponding realized stochastic system failure intensities and expected system failure intensity graphs. The parameter b governs

the percent of the initial failure intensity contributed by $\lambda_{(1)},\ldots,\lambda_{(k)}$. One can show $\eta(w)=\frac{1-b^w}{1-b^k}$ for $w=1,\ldots,k$. Also, holding λ and b fixed we obtain $\eta_\infty(w)=\lim_{k\to\infty}\eta(w)=1-b^w$ for $w=1,2,\ldots$.

As for the lognormal case, if $\eta(100)$ is lowered from its current value, then this will generally lead to the finite and infinite average of the PM2 MTBF planning curves being closer to the averages of the reciprocals of the realized and expected system failure intensities.

7. RELIABILITY GROWTH POTENTIAL.

7.1 Growth Potential in Terms of Planning Parameters.

In contrast to the MIL-HDBK-189 planning model, the PM2 planning approximation recognizes a ceiling for the MTBF. To obtain this limiting value we note that $\lim_{t\to\infty} h(t) = 0$. From Equation (26) we then obtain

$$\lim_{t\to\infty} \rho_{PL}(t) = (1-\mu_d)\cdot\lambda \tag{41}$$

This limiting value of $\rho_{PL}(t)$ is termed the growth potential failure intensity and is denoted by ρ_{GP}. The growth potential MTBF is defined to be $\rho_{GP}^{-1}(t)$ and is denoted by M_{GP}. Note,

$$M_{GP} = \frac{M_I}{1-\mu_d} \tag{42}$$

From Equation (30) it is clear that $\rho_{PL}(t)$ is a strictly decreasing function of *t* whose limit as $t\to\infty$ is ρ_{GP}. Equivalently, $MTBF_{PL}(t) = \rho_{PL}^{-1}(t)$ is a strictly increasing function of t whose limit as $t\to\infty$ is M_{GP}.

The above comments with respect to $\rho_{PL}(t)$ and $MTBF_{PL}(t)$ also apply to the case where failure modes are classified into A-modes and B-modes. However, for this case,

$$M_{GP} = \frac{M_I}{1-(MS)\cdot\mu_d'} \tag{43}$$

where μ_d' now denotes the average FEF with respect to the B-modes.

7.2 Planning Parameter β in Terms of Growth Potential.

The complex system planning formula for β, given by Equation (35), can be rewritten in terms of the MTBF growth potential. One can show,

$$\beta = \left(\frac{1}{T}\right)\left(\frac{\frac{M_G}{M_I}-1}{1-\frac{M_G}{M_{GP}}}\right) \tag{44}$$

This formula applies whether one or two failure mode categories are utilized, as long as the appropriate expression for M_{GP} is applied. For a logically consistent set of reliability growth planning parameters one must have $M_I < M_G < M_{GP}$. Note this ensures that $\beta > 0$.

7.3 Plausibility Metrics for Planning Parameters.

Observe that Equation (44) shows that if T is chosen to be unrealistically small for growing from M_I to M_G then the resulting value of β will be unduly large. This would be reflected in the function,

$$\theta(t) = \frac{\beta\cdot t}{1+\beta\cdot t} \tag{45}$$

rising towards one at an unrealistic rate. For example, a large β could imply that $\theta(t_0) = 0.80$ for an initial time segment $[0, t_0]$ for which past experience indicates it would not be feasible to surface a set of failure modes that accounted for 80% of the initial failure intensity. An unrealistically large β, and corresponding $\theta(t)$ function, could also arise by choosing M_G to be an excessively high percentage of M_{GP}. This discussion also pertains to the case where two failure mode categories are utilized. For this case $\theta(t)$ is replaced by $\theta_B(t)$, or the left-hand side of Equation (45). The value $\theta_B(t)$ denotes the expected fraction of λ_B attributed to the B-modes surfaced by t. The scale parameter β utilized in obtaining $\theta_B(t)$ is still given by Equation (44). However, to obtain $\theta_B(t)$, M_{GP} is computed via Equation (43).

A second potentially useful metric for judging whether the planning parameters give rise to a reasonable value for β is the implied average mode failure rate for the expected set of surfaced modes over a selected initial reference test period $[0, t_0]$. Denoting this average mode failure rate by $\rho_{avg}(t_0)$ we have,

$$\rho_{avg}(t_0) = \frac{\lambda - h(t_0)}{\mu(t_0)} \tag{46}$$

Classifying failure modes into A and B modes we have,

$$\rho_{avg,B}(t_0) = \frac{\lambda_B - h_B(t_0)}{\mu_B(t_0)} \tag{47}$$

where $\rho_{avg,B}(t_0)$ denotes the average B-mode failure rate for the set of B-modes expected to be surfaced during $[0, t_0]$. In Equation (47), $\mu_B(t_0)$ is the expected number of surfaced B-modes over $[0, t_0]$. For complex systems, Equation (46) yields,

$$\rho_{avg}(t_0) = \frac{(\beta \cdot t_0)^2}{t_0 \cdot (1 + \beta \cdot t_0) \cdot \ln(1 + \beta \cdot t_0)} \tag{48}$$

where β is given by Equation (44) with M_{GP} expressed by Equation (42). Likewise for complex systems, Equation (47) implies,

$$\rho_{avg,B}(t_0) = \frac{(\beta \cdot t_0)^2}{t_0 \cdot (1 + \beta \cdot t_0) \cdot \ln(1 + \beta \cdot t_0)} \tag{49}$$

where β is given by Equation (44) with M_{GP} expressed by Equation (44). For a given M_I (and MS for $\rho_{avg,B}(t_0)$), $\rho_{avg}(t_0)$ and $\rho_{avg,B}(t_0)$ can be expressed in terms of T and M_G for $M_I \le M_G < M_{GP}$. Denote these expressions for $\rho_{avg}(t_0)$ and $\rho_{avg,B}(t_0)$ by $\rho_{avg}(T, M_G; t_0)$ and $\rho_{avg}(T, M_G; t_0)$, respectively. The following properties of these functions can be useful in judging whether T and M_G are reasonable planning values:

1. $\rho_{avg}(T, M_G; t_0)$ and $\rho_{avg,B}(T, M_G; t_0)$ are continuous positive strictly decreasing functions of T and strictly increasing functions of M_G for $M_I \le M_G < M_{GP}$;
2. $\rho_{avg}(T, M_G; t_0)$ and $\rho_{avg,B}(T, M_G; t_0)$ approach infinity as T approaches zero or M_G approaches M_{GP} and;
3. $\rho_{avg}(T, M_G; t_0)$ and $\rho_{avg,B}(T, M_G; t_0)$ approach zero as T approaches infinity or M_G approaches M_I.

A third potentially useful metric to judge the reasonableness of the planning parameters is the expected number of unique failure modes or unique B-modes surfaced over an initial test interval $[0, t_0]$ they imply. Prior experience with similar developmental programs or initial data from the current program can serve as benchmarks.

8. GENERATING A PLANNED RELIABILITY GROWTH PATH.

Once the planning parameters are chosen, the parsimonious approximation for the expected failure intensity can be used to generate a detailed reliability growth planning curve. For example, suppose a test schedule is laid out that gives the planned number of RAM miles accumulated on the units under test per month. Also suppose the test schedule specifies blocks of calendar time for implementing corrective actions. Finally, for planning purposes let us assume that in order for a failure mode to be addressed in an upcoming corrective action period, it must occur four months prior to the start of the period. For this situation the MTBF could be represented by a constant value between the ends of corrective action periods and between the start of testing and the end of the first scheduled corrective action period (CAP). For such a test plan, jumps in MTBF would be portrayed at the conclusion of each CAP. The increased MTBF after the jump is given by $MTBF(t_i) = \{\rho(t_i)\}^{-1}$ where t_i denotes the accumulated test time, as determined from the monthly schedule, by the calendar date that occurs four months prior to the start of the ith CAP. Since $MTBF(t_i)$ depends on a large number of parameters it would be approximated by the parsimonious approximation $\{\rho_k(t_i)\}^{-1}$ or $\{\rho_\infty(t_i)\}^{-1}$. In such a manner a sequence of target MTBF steps would be generated that grow from the initial MTBF value to a goal MTBF value.

Figure 12 below depicts a detailed reliability growth planning curve for a complex system for the case where A and B failure mode categories are utilized.

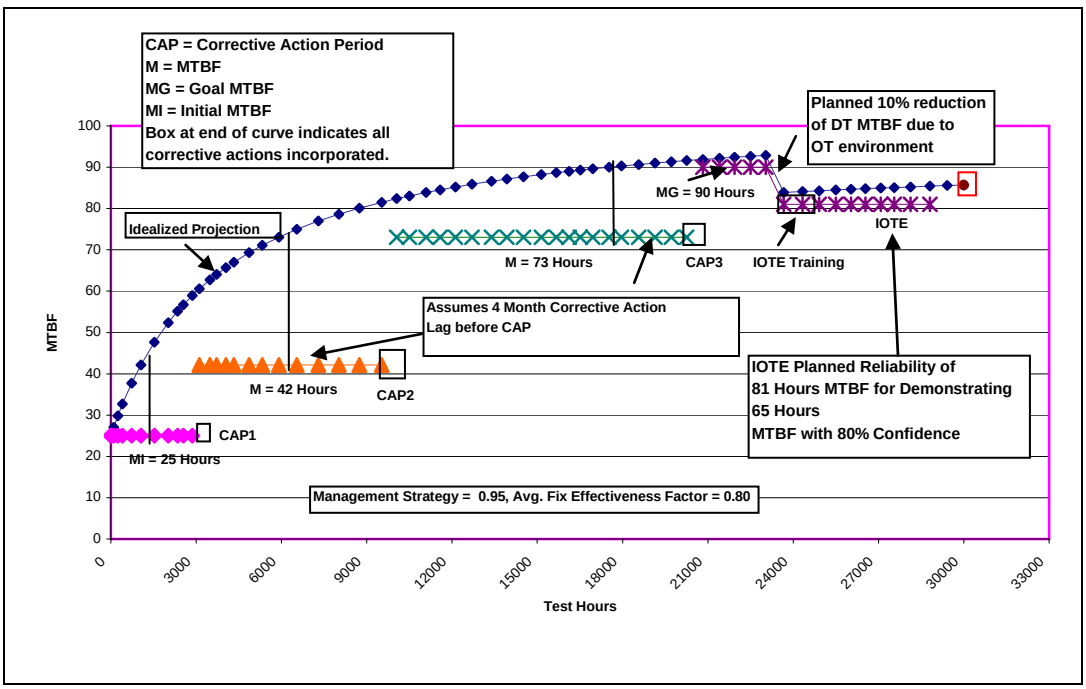

Figure 12. PM2 Reliability Growth Planning Curve.

The blue curve in Figure 12 represents $MTBF(t) = \{\rho_{PL}(t)\}^{-1}$ where $\rho_{PL}(t)$ is given by Equation (36) and β is obtained from the planning parameters by Equation (37). Note the value $MTBF(t)$ is the system MTBF one expects to obtain once all corrective actions to B-

modes surfaced during test period $[0,t]$ are implemented. The MTBF steps are constructed from the blue curve, the schedule of corrective action periods (CAPs), and the assumed average corrective action implementation lag. In Figure 12 note that the goal MTBF, M_G, was chosen to be larger than $M_R = 65$ hours, the MTBF to be demonstrated during a follow-on Initial Operational Test and Evaluation (IOT&E). This test is an operational demonstration test of the system's suitability for fielding. Such a test is mandated by public law for major DoD developmental systems. In such a demonstration test it may be required to demonstrate M_R with a measure of assurance. In the figure we have utilized as our measure of assurance a demonstration of M_R at the 80% statistical confidence level. To have a reasonable probability of achieving such a demonstration, the system must enter the IOT&E with an MTBF value of M_R^+ which is greater than M_R. The needed value of M_R^+ can be determined by a well-known statistical procedure from the IOT&E test length, the desired confidence level of the statistical demonstration, and the specified probability of being able to achieve the statistical demonstration. After determining M_R^+ one can consider what the goal MTBF, M_G, should be at the conclusion of the development test. The value of M_G should be the goal MTBF to be attained just prior to the IOT&E training period that proceeds the IOT&E. The goal MTBF associated with the development test environment must be chosen sufficiently above M_R^+ so that the operational test environment does not cause the reliability of the test units to fall below M_R^+ during the IOT&E. The significant drop in MTBF often seen could be attributable to operational failure modes that were not encountered during the developmental test. In Figure 12 a derating factor of 10% was used to obtain M_G from M_R^+, i.e., in the figure $M_G = \frac{M_R^+}{0.90}$.

REFERENCES

1. Boyce, W.E., and DiPrima, R.C., "*Elementary Differential Equations and Boundary Value Problems*," John Wiley & Sons, Inc., New York, 1965.

2. Broemm, W.J., Ellner, P.M., Woodworth, W.J., "AMSAA Reliability Growth Guide," *AMSAA TR-652*, (September) 2000.

3. Crow, L.H., "An Improved Methodology for Reliability Growth Projections," *AMSAA TR-357*, (June) 1982.

4. Crow, L.H., "An Extended Reliability Growth Model for Managing and Assessing Corrective Actions," *Proceedings of the Reliability and Maintainability Symposium*, 2004.

5. Department of Defense, "Reliability Growth Management," *MIL-HDBK-189*, Washington, DC, (February) 1981.

6. Duane, J.T., "Learning Curve Approach to Reliability Monitoring," *IEEE Transactions on Aerospace*, Vol. 2, No. 2, (April) 1964.

7. Ellner, P.M., and Hall, J.B., "The AMSAA Maturity Projection Model based on Stein Estimation," *AMSAA TR-751*, (July) 2004.

8. Fakhre-Zakeri, I., and Slud, E., "Models of Empirical-Bayes Type for Software Reliability: Identifiably and Applications to Optimal Stopping of Software Testing," University of Maryland TR-MD92-12-IFZ-ES, 1992.

9. Meeker, W.Q., and Escobar, L.A., "*Statistical Methods for Reliability Data*," John Wiley & Sons, Inc., New York, 1998.

10. Miller, D.R., "Exponential Order Statistic Models of Software Reliability Growth," *NASA CR- 3909*, 1985.

11. Nagel, P.M., Scholz, F.W., and Skrivan, J.A., "Software Reliability: Additional Investigations into Modeling with Replicated Experiments," *NASA CR-172378*, 1984.

12. Nagel, P.M., and Skrivan, J.A., "Software Reliability: Repetitive Run Experiment and Modeling," *NASA CR-165836*, 1982.

THIS PAGE IS INTENSIONALLY LEFT BLANK.

APPENDIX A - SIMULATION

THIS PAGE IS INTENSIONALLY LEFT BLANK.

A. SIMULATION.

A.1 Simulating a Developmental Test.

The first part of the simulation generates data typical to that which would be captured during a developmental test. There are a number of inputs to the simulation. A variety of parent populations of initial mode failure rates are explored. The failure rates are either deterministically calculated, or stochastically generated. The deterministic failure rates are calculated in accordance to a specified geometric sequence. The choice of stochastic parent populations of failure rates include: (1) gamma; (2) lognormal; (3) Weibull or; (4) log logistic. Using the failure rates, the failure mode First Occurrence Times (FOTs) are calculated. Using the mode failure rates in addition to the FOTs, the remaining mode failure times in the test are generated. Failure mode Fix Effectiveness Factors (FEFs) are drawn from a beta distribution with mean 0.8 and a coefficient of variation of 0.1. The simulation is replicated a specified number of times. The failure rates, failure times, and FEFs produced during each replication are saved.

```
(*** INPUTS *)
<< Statistics`
<< Graphics`
VGS = 1;
BetaAlternate = 0;
Deterministic = 0;
PM2[] := {
   dist = 2; (* 1-Gamma, 2-Log Normal, 3-Weibull, 4-LogLogistic *)
   β_a = {0.0001, 0.001};
   T = 10000;
   k_A = 5;
   k_B = 1500;
   Eλ_{A,K} = 10^-1;
   Eλ_{B,K} = 10^-1;
   α_a = {Eλ_{A,K}/(k_A β_a[[1]]), Eλ_{B,K}/(k_B β_a[[2]])};

   (*** DISTRIBUTION PARAMETERS *)
   σ_n = Sqrt[Log[1 + 1/α_a]];
   μ_n = Log[α_a β_a / Sqrt[1 + 1/α_a]];
   β_w = {x /. FindRoot[Gamma[1 + 2/x] / Gamma[1 + 1/x]^2 == 1 + 1/α_a[[1]], {x, .5}],
```

```
  x /. FindRoot[Gamma[1 + 2/x] / Gamma[1 + 1/x]^2 == 1 + 1/α_a[[2]], {x, .5}]};
θ_w = α_a β_a / Gamma[1 + 1/β_w];
σ_ln = {σ_l /. FindRoot[Gamma[1 - 2 σ_l] Gamma[1 + 2 σ_l] / (Gamma[1 - σ_l]^2 Gamma[1 + σ_l]^2) == 1 + 1/α_a[[1]], {σ_l, .1}],
  σ_l /. FindRoot[Gamma[1 - 2 σ_l] Gamma[1 + 2 σ_l] / (Gamma[1 - σ_l]^2 Gamma[1 + σ_l]^2) == 1 + 1/α_a[[2]], {σ_l, .1}]};
μ_ln = Log[α_a β_a / (Gamma[1 + σ_ln] Gamma[1 - σ_ln])];
GammaMean = Mean[GammaDistribution[α_a[[2]], β_a[[2]]]];
GammaVariance = Variance[GammaDistribution[α_a[[2]], β_a[[2]]]];

(*** A & B-MODE FAILURE RATES *)
If[Deterministic == 1,
 βoverλ = 0.01;
 λ_K = 0.1;
 c = (βoverλ + 1) / (1 - βoverλ);
 b = b /. FindRoot[c == (1 - b^(k_B+1)) / (b - b^k_B), {b, 0.8}];
 a = ((1 - b) / (1 - b^k_B)) λ_K;
 λ_A = Table[a b^(i-1), {i, k_A}];
 λ_B = Table[a b^(i-1), {i, k_B}];,

 λ_A = Which[
   dist == 1, Table[Random[GammaDistribution[α_a[[1]], β_a[[1]]]], {i, k_A}],
   dist == 2, Table[Random[LogNormalDistribution[μ_n[[1]], σ_n[[1]]]], {i, k_A}],
   dist == 3, Table[Random[WeibullDistribution[β_w[[1]], θ_w[[1]]]], {i, k_A}],
   dist == 4, Table[e^Random[LogisticDistribution[μ_ln[[1]], σ_ln[[1]]]], {i, k_A}]];
 If[Length[Position[λ_A, 0.]] > 0,
  λ_A = ReplacePart[λ_A, 10^-10, Position[λ_A, 0.]], (* Do Nothing *)];
 λ_B = Which[
   dist == 1, Table[Random[GammaDistribution[α_a[[2]], β_a[[2]]]], {i, k_B}],
   dist == 2, Table[Random[LogNormalDistribution[μ_n[[2]], σ_n[[2]]]], {i, k_B}],
   dist == 3, Table[Random[WeibullDistribution[β_w[[2]], θ_w[[2]]]], {i, k_B}],
   dist == 4, Table[e^Random[LogisticDistribution[μ_ln[[2]], σ_ln[[2]]]], {i, k_B}]];
 If[Length[Position[λ_B, 0.]] > 0,
  λ_B = ReplacePart[λ_B, 10^-10, Position[λ_B, 0.]], (* Do Nothing *)];]

(*** UNIFORM RANDOM NUMBERS *)
U_A = Table[Random[], {i, k_A}];
U_B = Table[Random[], {i, k_B}];

(*** FIRST OCCURRENCE TIMES *)
t_A = -Log[U_A] / λ_A;
```

```
t_B = -Log[U_B] / λ_B;

(*** FIX EFFECTIVENESS FACTORS *)
c = 0.8;
v = 0.1;
q = (1 - c - c v^2) / v^2;
r = ((1 - c) / c) q;
d_A = Table[0, {i, k_A}];
d_B = Table[Random[BetaDistribution[q, r]], {i, k_B}];

(*** FAILURE TIMES *)
timeline[tlist_, λlist_, dlist_] := {
  tl = Table[If[tlist[[i]] ≤ T, {tlist[[i]]}, Null], {i, Length[tlist]}];
  Table[While[Max[tl[[i]]] ≤ T,
     NewT = Max[tl[[i]]] - Log[Random[]] / ((1 - dlist[[i]]) λlist[[i]]);
     If[NewT ≤ T, AppendTo[tl[[i]], NewT], Break[]];
    ];, {i, 1, Length[tlist]}]; tl};
x = Sort[Flatten[Cases[Flatten[timeline[t_B, λ_B, d_B], 1], _List]]];

(*** DATA STORAGE *)
AppendTo[ReplicatedFailureRates, λ_B];
AppendTo[ReplicatedFailureTimes, x];
AppendTo[ReplicatedFOT, t_B];
AppendTo[ReplicatedFEF, d_B];};
```

A.2 Replicating the Simulation.

The code in the previous section defined a function PM2[], which simulates data typical to that which would follow from developmental testing. The code below executes the simulation for a specified number of replications. Only one replication is required when using deterministic failure rates, since they are calculated in accordance with a geometric sequence. That is, there is no variability in the failure rates in the deterministic case from replication to replication. Note though that FEFs are generated during each replication of the simulation.

```
ReplicatedFailureRates = {};
ReplicatedFailureTimes = {};
ReplicatedFOT = {};
ReplicatedFEF = {};
Replications = If[Deterministic == 1, 1, 10];
Table[PM2[], {Replications}];
```

A.3 Input Parameters, and Distributions.

This section prints a summary of the input parameters utilized in the simulation. The inputs include the number of replications, the test length, the parent population of failure rates, the number of potential A-modes, and the number of potential B-modes. Simulation results; such as, the average number of surfaced failure modes, the average number of failures, the average estimated growth rate, and MLEs for the distribution parameters are also printed. A plot of there Probability Density Functions (PDFs) of the various parent populations of initial mode failure rates is displayed in Figure 13.

```
(*** INPUTS *)
ReplicatedSurfaced =
  Table[Length[Position[ReplicatedFOT[[i]], _?(# ≤ T &)]], {i, 1, Replications}];
ReplicatedFailures = Map[Length[#] &, ReplicatedFailureTimes];
β_crow = Map[((Length[#] - 1)/Length[#]) Length[#]/(Sum_{i=1}^{Length[#]} Log[T/#[[i]]]) &, ReplicatedFailureTimes];
Print["SIMULATION INPUTS:\n",
  "Replications : " <> ToString[Replications],
  "\nTest Length  : " <> ToString[T],
  "\nFailure Rates: " If[Deterministic == 1, "Geometric", Which[dist == 1, "Gamma",
     dist == 2, "Log Normal", dist == 3, "Weibull", dist == 4, "LogLogistic"]],
  "\nA-Modes : " <> ToString[k_A],
  "\nB-Modes : " <> ToString[k_B],
  "\nSurfaced: " <> ToString[Ceiling[Mean[ReplicatedSurfaced]]],
  "\nFailures: " <> ToString[Ceiling[Mean[ReplicatedFailures]]],
  "\nGrowth Rate: " <> ToString[Mean[1 - β_crow]]];

(*** DISTRIBUTIONS *)
Print["DISTRIBUTION PARAMETERS:\n",
 TableForm[{
   {"Gamma", "Normal", "Weibull", "Logistic"},
   {"β= " <> ToString[NumberForm[β_a[[2]], {6, 4}, NumberPadding → {"", "0"}]],
    "μ= " <> ToString[NumberForm[μ_n[[2]], {6, 2}, NumberPadding → {"", "0"}]],
    "β= " <> ToString[NumberForm[β_w[[2]], {6, 4}, NumberPadding → {"", "0"}]],
    "μ= " <> ToString[If[
       TrueQ[Head[μ_ln[[2]]] == Complex || Head[σ_ln[[2]]] == Complex],
       "DNE",
       NumberForm[μ_ln[[2]], {6, 2}, NumberPadding → {"", "0"}]]]},
   {"α= " <> ToString[NumberForm[α_a[[2]], {6, 4}, NumberPadding → {"", "0"}]],
    "σ= " <> ToString[NumberForm[σ_n[[2]], {6, 4}, NumberPadding → {"", "0"}]],
    "θ= " <> ToString[NumberForm[θ_w[[2]], {6, 4},
       NumberPadding → {"", "0"}, ExponentFunction → (Null &)]],
    "σ= " <> ToString[If[
       TrueQ[Head[μ_ln[[2]]] == Complex || Head[σ_ln[[2]]] == Complex],
       "DNE", NumberForm[σ_ln[[2]], {6, 4}, NumberPadding → {"", "0"}]]]}}],
 "\nMean = " <> ToString[GammaMean],
 "\nVariance = " <> ToString[NumberForm[GammaVariance, ExponentFunction → (Null &)]]]
```

```
(*** PDF PLOTS *)

LogLogisPDF[x_, μ_, σ_] := 1/(σ x) (e^((Log[x]-μ)/σ)/(1 + e^((Log[x]-μ)/σ))^2);

Plot[{
   PDF[GammaDistribution[αa[[2]], βa[[2]]], x],
   PDF[LogNormalDistribution[μn[[2]], σn[[2]]], x],
   PDF[WeibullDistribution[βw[[2]], θw[[2]]], x],
   If[
    TrueQ[Head[μln[[2]]] == Complex], 1, LogLogisPDF[x, μln[[2]], σln[[2]]]]
  }, {x, 0, 2 Mean[GammaDistribution[αa[[2]], βa[[2]]]]},
  Frame → True, FrameLabel → {"Failure Rate", "PDF"},
  PlotStyle → {Hue[1], Hue[.7], Hue[.35], Hue[.5]},
  PlotLegend → {"Gamma", "LogNormal", "Weibull", "LogLogistic"},
  LegendPosition → {.9, -.3}, LegendTextSpace → 4];
```

```
SIMULATION INPUTS:
Replications : 10
Test Length  : 10000
Failure Rates:  Log Normal
A-Modes : 5
B-Modes : 1500
Surfaced: 395
Failures: 514
Growth Rate: 0.195564

DISTRIBUTION PARAMETERS:
 Gamma          Normal         Weibull        Logistic
β= 0.0010       μ= -11.00      β= 0.3548      μ= -10.04
α= 0.0667       σ= 1.6651      θ= 0.0000      σ= 0.4870
Mean = 0.0000666667
Variance = 0.0000000666667
```

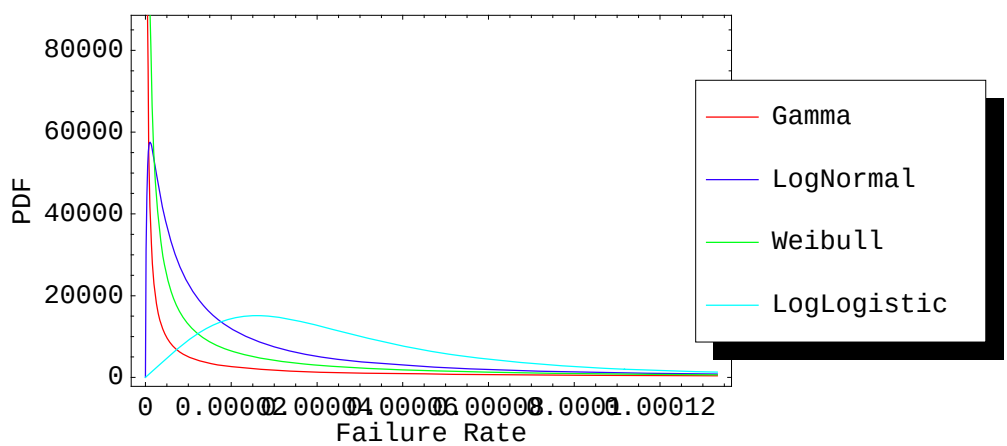

Figure 13. Failure Rate Parent Populations.

From the data above, we can see that 10 developmental tests of length 10,000 hours have been simulated. In each replication, 5 A-modes and 1,500 B-modes are generated from a lognormal parent population. An average number of 395 failure modes, and 514 failures were surfaced over the 10 replicated tests. The average growth rate over the 10 tests was approximately 0.2. Note that the estimate of the growth rate is based on the AMSAA-Crow model. Figure 13 shows the PDFs for the various parent populations for which failure rates can be drawn. Studying various parent populations is important in examining how robust the PM2 model is with respect to the assumption that the initial mode failiure rates constitute a realization of a random sample from a gamma random variable.

A.4 Visual Growth Suite.

The simulation contains an option to either calculate the reliability projections using individual mode failure rates, or utilize the AMSAA Growth Guide (Ellner et al., 2000) methodology. If the methodology in the growth guide is used, the following code will estimate the scale and shape paremeters of the gamma distribution in two cases. The first case is when the number of failure modes is known or assumed. The second case estimates the limiting form of the parameters (i.e. as the number of failure modes k→∞).

```
(* VGS Parameter Estimates *)
Off[FindRoot::"lstol", FindRoot::"frmp"]
If[VGS == 1,
  m = ReplicatedSurfaced;
  Clear[x];
  SurfacedFOT = Map[Extract[#, Position[#, _?(# ≤ T &)]] &, ReplicatedFOT];

  (* BETA INFINITE *)
  BetaInf = If[BetaAlternate == 1,
    g[x_] = Table[x Sum[x SurfacedFOT[[j]][[i]] / (1 + x SurfacedFOT[[j]][[i]]), {i, 1, m[[j]]}] +
       Total[ReplicatedFailureRates[[j]]] (x T / (1 + x T) - Log[1 + x T]), {j, 1, Replications}];
    Map[x /. FindRoot[# == 0, {x, β_a[[2]]}] &, g[x]],

    f[x_] =
     Table[{Log[1 + x T] Sum[(1 / (1 + x SurfacedFOT[[j]][[i]])), {i, 1, m[[j]]}] - m[[j]] x T / (1 + x T)}, {j, 1, Replications}];
    Map[x /. FindRoot[# == 0, {x, β_a[[2]] / 2}] &, f[x]]];
  Clear[f, g];
  (* BETA FINITE *)
  BetaFinite = If[BetaAlternate == 1,
    f[x_] = Table[
      x Sum[x SurfacedFOT[[j]][[i]] / (1 + x SurfacedFOT[[j]][[i]]), {i, 1, m[[j]]}] + Total[ReplicatedFailureRates[[j]]] / k_B
```

```
      Sum[(x SurfacedFOT[[j]][[i]] / (1 + x SurfacedFOT[[j]][[i]]) - Log[1 + x SurfacedFOT[[j]][[i]]]), {i, 1, m[[j]]}] +
      (1 - m[[j]] / k_B) Total[ReplicatedFailureRates[[j]]] (x T / (1 + x T) - Log[1 + x T])
    , {j, 1, Replications}];
  Table[x /. FindRoot[f[x][[i]] == 0, {x, BetaInf[[i]]}], {i, 1, Replications}],
  g[x_] = Table[((Sum[Log[(1 + x T) / (1 + x SurfacedFOT[[j]][[i]])], {i, 1, m[[j]]}]) (Sum[1 / (1 + x SurfacedFOT[[j]][[i]]), {i, 1, m[[j]]}]) -
        (m[[j]] x / (1 + x T)) (Sum[(T - SurfacedFOT[[j]][[i]]) / (1 + x SurfacedFOT[[j]][[i]]), {i, 1, m[[j]]}])) /
      (Log[1 + x T] (Sum[1 / (1 + x SurfacedFOT[[j]][[i]]), {i, 1, m[[j]]}]) - (m[[j]] x / (1 + x T)) T), {j, 1, Replications}];
  Map[x /. FindRoot[# == k_B, {x, BetaInf[[1]] / 2}] &, g[x]]];

(* ALPHA PLUS ONE *)
AlphaPlusOne = If[BetaAlternate == 1,
  Map[Total[#] &, ReplicatedFailureRates] / (k_B BetaFinite),
  Table[(m[[j]] / BetaFinite[[j]] - Sum[SurfacedFOT[[j]][[i]] / (1+BetaFinite[[j]] SurfacedFOT[[j]][[i]]), {i=1, m[[j]]}]) / ((k_B-m[[j]]) T / (1+BetaFinite[[j]] T) + Sum[SurfacedFOT[[j]][[i]] / (1+BetaFinite[[j]] SurfacedFOT[[j]][[i]]), {i=1, m[[j]]}]), {j, 1, Replications}]];
(* LAMBDA INFINITE *)

LambdaInf =
 If[BetaAlternate == 1, Map[Total[#] &, ReplicatedFailureRates],
  Table[m[[j]] BetaInf[[j]] / Log[1 + BetaInf[[j]] T], {j, 1, Replications}]];

(* LAMBDA FINITE *)
LambdaFinite = If[BetaAlternate == 1, Map[Total[#] &, ReplicatedFailureRates],
  Table[k_B BetaFinite[[j]] AlphaPlusOne[[j]], {j, 1, Replications}]];

(* VGS DATA *)
VGSdata = Transpose[{BetaInf, BetaFinite, AlphaPlusOne, LambdaInf, LambdaFinite}];
Print[TableForm[VGSdata, TableHeadings → {Automatic, {"β∞", "βk", "α+1", "λ∞", "λk"}}]]
, Print["Option Not Used."]];
```

	β_∞	β_k	α+1	λ_∞	λ_k
1	0.0002724	0.000172801	0.306968	0.0824577	0.0795666
2	0.000288045	0.000187303	0.294969	0.0851845	0.0828727
3	0.00034043	0.000227366	0.254715	0.0897813	0.0868701
4	0.000257505	0.000164339	0.316343	0.0802443	0.0779812
5	0.000284446	0.000181452	0.291483	0.08259	0.0793353
6	0.000208522	0.000125068	0.380843	0.0738492	0.0714471
7	0.000312976	0.000199775	0.275441	0.0865075	0.0825396
8	0.0002851	0.000179283	0.314487	0.0875388	0.0845734
9	0.000367495	0.000252826	0.231049	0.0903118	0.0876227
10	0.000374229	0.000246748	0.23718	0.0923239	0.0877856

Table 1. Visual Growth Suite Parameter MLEs.

Table 1 displays MLEs of five parameters, β_∞, β_k, α+1, λ_∞, and λ_k over 10 replications of the simulation. β_∞ is the MLE of the shape parameter of the gamma distribution in the limiting case (as the number of failure modes approaches infinity). β_k is the MLE of the gamma shape parameter for a finite number of failure modes. α+1 is the MLE for the gamma scale parameter for finite k. The MLEs of the initial system B-Mode failure intensity is given by λ_∞ and λ_k for an infinite and finite number of modes, respectively.

A.5 Average Number of Failure Modes Surfaced.

The average number of failure modes surfaced over the test is examined using all the data generated over the replicated simulation runs. There are four series plotted in Figure 14 below. The black dots represent the actual average number of modes surfaced. The red line is the expected value of the number of surfaced failure modes. The green line is the PM2 estimate of the average number of surfaced modes using a finite number of modes. The blue line is the PM2 estimate of the average number of surfaced modes using an infinite number of modes.

```
(*** SURFACED B-MODES *)
SurfacedModes = {};
Table[
  NBM = {};
  steps = {};
  Table[
   SBMp = Position[ReplicatedFOT[[i]], _?(# ≤ tp &)];
   AppendTo[NBM, Length[SBMp]];
   AppendTo[steps, tp];, {tp, 50, T, 1000}];
  AppendTo[SurfacedModes, NBM];, {i, 1, Replications}];

(*** AVG. NUMBER OF MODES SURFACED PLOT *)
(*** ACTUAL *)
Actual = ListPlot[
   Transpose[{steps, Mean[SurfacedModes]}], Frame → True,
   FrameLabel → {"Test Time", "Avg. Surfaced"},
   PlotRange → {0, 1.25 Max[Map[Max[#] &, SurfacedModes]]},
```

```
   PlotStyle → {PointSize[0.01]}, Background → GrayLevel[0.8],
   GridLines → Automatic, DisplayFunction → Identity];

(*** FINITE *)
Exact = Plot[Mean[Map[{k_B - Sum[e^(-#[[i]] t), {i, 1, k_B}]} &, ReplicatedFailureRates]], {t, 1, T},
   PlotStyle → Hue[1], DisplayFunction → Identity];
Finite = If[VGS == 1,
   Plot[Mean[k_B (1 - (1/(1 + BetaFinite t))^AlphaPlusOne)],
    {t, 1, T}, PlotStyle → Hue[.35], DisplayFunction → Identity],
   Plot[Mean[Map[{k_B (1 - (1/(1 + ((Sum[#[[i]]^2, {i, 1, k_B}]/Total[#] - Total[#]/k_B)/(1 - 1/k_B)) t))^((1/k_B (1 - 1/k_B) Total[#])/(Sum[#[[i]]^2, {i, 1, k_B}]/Total[#] - Total[#]/k_B)))} &, ReplicatedFailureRates]]
    {t, 1, T}, PlotStyle → Hue[.35], DisplayFunction → Identity]];

(*** INFINITE *)
Inf = If[VGS == 1,
   Inf = Plot[Mean[(LambdaInf/BetaInf) Log[1 + BetaInf t]],
     {t, 1, T}, PlotStyle → Hue[.6], DisplayFunction → Identity],
   Plot[Mean[Map[{(Total[#]/((Sum[#[[i]]^2, {i, 1, k_B}]/Total[#]))) Log[1 + (Sum[#[[i]]^2, {i, 1, k_B}]/Total[#]) t]} &, ReplicatedFailureRates]],
    {t, 1, T}, PlotStyle → Hue[.6], DisplayFunction → Identity]];

Show[{Actual, Exact, Finite, Inf}, DisplayFunction → $DisplayFunction];
```

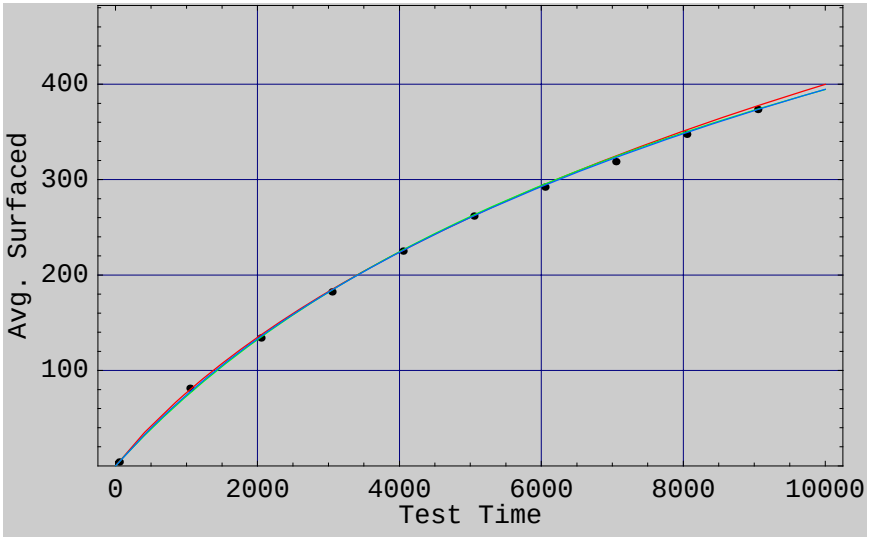

Figure 14. Average Number of Modes Surfaced.

Notice from Figure 14 that the various PM2 estimates of the average number of surfaced failure modes over the test phase are highly accurate in comparison to the black dots (i.e. the actual averge number of surfaced modes). Also note that this accuracy is achieved when violating the PM2 assumption that the failure rates are gamma distributed. That is, in this sequence of replications, failure rates were drawn from a lognormal distribution.

A.6 Failure Mode Profile.

Figure 15 below is a plot of the failure mode profile. The profile is a plot of the magnitude of the simulated failure rates in decending order. This provides a graphical indication of the shape of the distribution.

```
ListPlot[data, PlotRange → All, Frame → True,
  FrameLabel → {"Mode", "Mode Failure Rate"}, GridLines → Automatic];
```

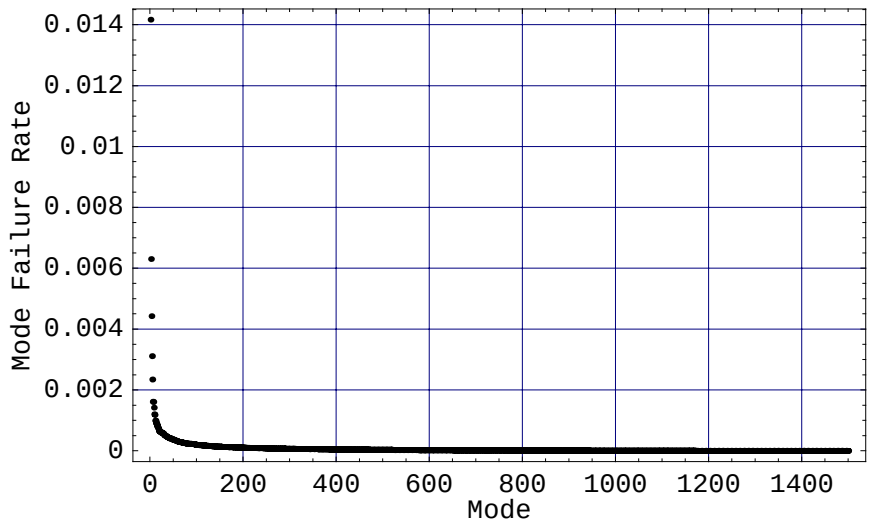

Figure 15. Failure Mode Profile.

A.7 Cumulative Failure Mode Profile.

Figure 16 below displays a plot of the cumulative failure mode profile. This profile is important in understanding the impact of the top "w" failure modes. For example, slightly over 60% of the system failure rate is contained within the top 100 failure modes in this particular sequence of simulation replications.

```
Clear[λ];
data = Sort[λB, Greater];
Plot[Sum[data⟦i⟧, {i, j}] / Total[λB], {j, 1, kB},
  PlotRange → {{0, 1.25 Max[Map[Max[#] &, SurfacedModes]]}, All},
  Frame → True, FrameLabel → {"Number of Modes", "% of Top W Modes"},
  GridLines → Automatic];
TableForm[Table[{j, Sum[data⟦i⟧, {i, j}] / Total[λB]}, {j, 1, kB}]];
```

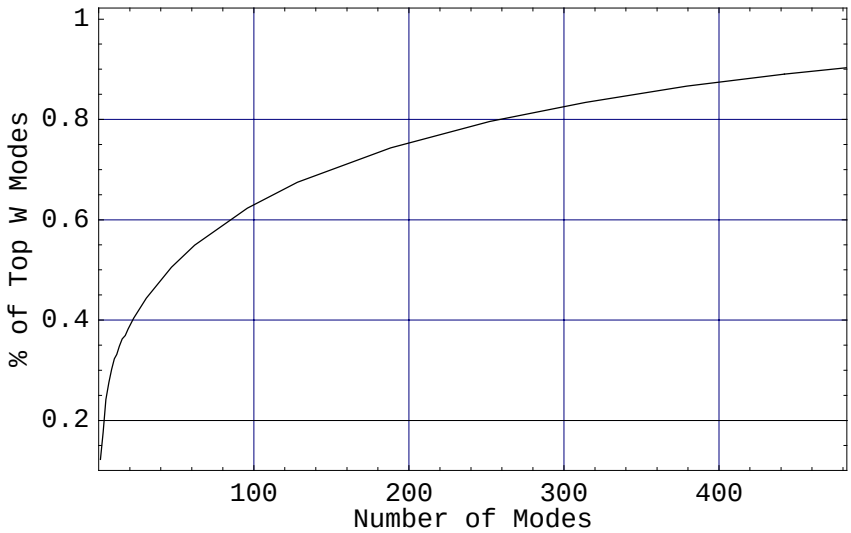

Figure 16. Cumulative Failure Mode Profile.

A.8 System Mean Time between Failure.

The system MTBF is examined in Figure 17 below. The black dots represent the actual MTBF which is known since the failure rates are generated during the simulation. The red line is the reciprocal of the expected system failure intensity. The green line is the PM2 estimate of the MTBF using a finite number of modes, and the blue line is the PM2 estimate of the MTBF for an infinite number of modes. The yellow curve is the esimate of the system MTBF provided by the AMSAA-Crow model. In Figure 17 the blue and green series are statistically fit to the surfaced number of modes using MLEs based on first occurrence time data. The yellow curve is statistically fit using all failure data (i.e., first occurrence times and the number of failures for each mode). MTBF curves will also be constructed from planning curves (i.e., not statistically fit) in Section A.11 of this report.

```
(*** ACTUAL - BLACK DOTS *)
ActualFR = Table[
   FailureRateData = {};
   Table[
    SurfacedModes = Position[ReplicatedFOT⟦i⟧, _?(# ≤ t &)];
    m = Length[SurfacedModes];
```

```
    ρ = Sum[((1 - Extract[ReplicatedFEF[[i]], SurfacedModes][[j]])
          Extract[ReplicatedFailureRates[[i]], SurfacedModes][[j]]) +
        Sum[Delete[ReplicatedFailureRates[[i]], SurfacedModes][[j]], {j, 1, k_B - m}]
    AppendTo[FailureRateData, ρ];
    , {t, 50, T, 1000}];
   FailureRateData, {i, 1, Replications}];
AverageActualFR = Mean[ActualFR];
Actual = ListPlot[Transpose[{steps, 1 / AverageActualFR}],
   Frame → True, FrameLabel → {"Test Time", "MTBF"},
   PlotRange → {0, 1.25 Max[1 / AverageActualFR]},
   GridLines → Automatic, PlotStyle → PointSize[.01],
   Background → GrayLevel[0.8], DisplayFunction → Identity];

(*** EXACT - RED LINE *)
Clear[ρ];
h_E[t_] = Table[λ_B = ReplicatedFailureRates[[i]]; {Sum[λ_B[[j]] e^(-λ_B[[j]] t), {j, 1, k_B}]}, {i, 1, Replications}];
ρ_E[t_] = Table[
   λ_B = ReplicatedFailureRates[[i]];
   d_B = ReplicatedFEF[[i]];
   {Sum[(1 - d_B[[j]]) λ_B[[j]], {j, 1, k_B}] + Sum[d_B[[j]] λ_B[[j]] e^(-λ_B[[j]] t), {j, 1, k_B}]}, {i, 1, Replications}];
Exact = Plot[Mean[1 / ρ_E[t]], {t, 0, T},
   PlotStyle → Hue[1], Frame → True,
   FrameLabel -> {"Test Time", "Exact MTBF"},
   PlotRange → All, GridLines → Automatic, DisplayFunction → Identity];

(*** FINITE CASE - GREEN LINE *)
λ = Map[Total[#] &, ReplicatedFailureRates];
β_K = Map[((1/Total[#]) Total[#^2] - Total[#]/k_B) / (1 - 1/k_B) &, ReplicatedFailureRates];
p_K = λ / (k_B β_K);
h_K[t_] = If[VGS == 1, LambdaFinite / (1 + t BetaFinite)^(AlphaPlusOne+1), λ / (1 + t β_K)^(p_K+1)];
μ_d = Map[Mean[#] &, ReplicatedFEF];
ρ_K[t_] = If[VGS == 1,
   (1 - μ_d) (LambdaFinite - LambdaFinite / (1 + t BetaFinite)^(AlphaPlusOne+1)) + LambdaFinite / (1 + t BetaFinite)^(AlphaPlusOne+1),
   (1 - μ_d) (λ - h_K[t]) + h_K[t]];

Finite = Plot[Mean[1 / ρ_K[t]], {t, 0, T},
   PlotStyle → Hue[0.35], Frame → True,
   FrameLabel -> {"Test Time", "Exact MTBF"},
```

```
(*** INFINITE CASE - BLUE LINE *)
βK = Map[Total[#^2]/Total[#] &, ReplicatedFailureRates];
h∞[t_] = If[VGS == 1, LambdaInf/(1 + t BetaInf), λ/(1 + t βK)];
ρ∞[t_] = If[VGS == 1,
   (1 - μd) (LambdaInf - LambdaInf/(1 + t BetaInf)) + LambdaInf/(1 + t BetaInf), (1 - μd) (λ - h∞[t]) + h∞[t]];
Inf = Plot[Mean[1 / ρ∞[t]], {t, 0, T},
   PlotStyle → Hue[0.6], Frame → True,
   FrameLabel -> {"Test Time", "Exact MTBF"},
   PlotRange → All, GridLines → Automatic, DisplayFunction → Identity];

(*** CROW *)
λcrow = ReplicatedFailures/T^βcrow;
μcrow[t_] = Mean[λcrow t^βcrow];
ρcrow[t_] := Mean[λcrow βcrow t^(βcrow-1)];
LC = Plot[1 / ρcrow[t], {t, 0, T},
   PlotStyle → Hue[0.15], Frame → True,
   FrameLabel -> {"Test Time", "Exact MTBF"},
   PlotRange → All, GridLines → Automatic, DisplayFunction → Identity];

Show[{Actual, Exact, Finite, Inf, LC}, DisplayFunction → $DisplayFunction];
```

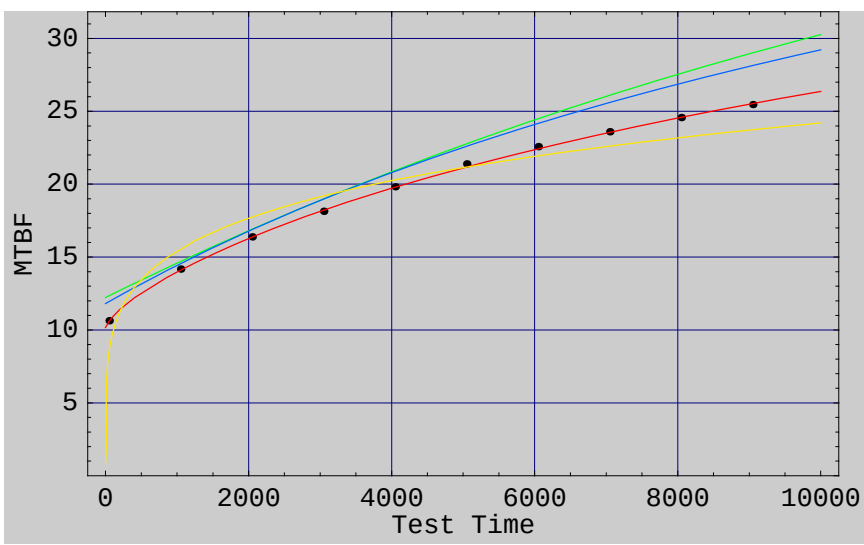

Figure 17. System MTBF.

A.9 System Failure Intensity.

The system failure intensity is plotted and displayed in Figure 18 below. The black dots represent the actual system failure intensity which is known since the failure rates are simulated. The red line is the expected system failure intensity. The green line is the PM2 estimate of the failure intensity using a finite number of modes, and the blue line is the PM2 estimate of the failure intensity for an infinite number of modes. The yellow curve is the esimate of the system failure intensity provided by the AMSAA-Crow model.

```
(*** ACTUAL - BLACK DOTS *)
Actual = ListPlot[Transpose[{steps, AverageActualFR}],
   Frame → True, FrameLabel → {"Test Time", "Failure Rate"},
   PlotRange → {0, Max[AverageActualFR]}, GridLines → Automatic,
   PlotStyle → PointSize[0.01],
   Background → GrayLevel[0.8], DisplayFunction → Identity];

(*** CROW *)
LC = Plot[ρcrow[t], {t, 0, T}, PlotStyle → Hue[0.15],
   Frame → True, FrameLabel -> {"Test Time", "Exact Failure Rate"},
   PlotRange → All, GridLines → Automatic, DisplayFunction → Identity];

(*** EXACT - RED LINE *)
Exact = Plot[Mean[ρE[t]], {t, 0, T},
   PlotStyle → Hue[1], Frame → True,
   FrameLabel -> {"Test Time", "Exact Failure Rate"},
   PlotRange → All, GridLines → Automatic, DisplayFunction → Identity];

(*** FINITE - GREEN LINE *)
Finite = Plot[Mean[ρK[t]], {t, 0, T},
   PlotStyle → Hue[0.35], Frame → True,
   FrameLabel -> {"Test Time", "Exact MTBF"},
   PlotRange → All, GridLines → Automatic, DisplayFunction → Identity];

(*** INFINITE - BLUE LINE *)
Inf = Plot[Mean[ρ∞[t]], {t, 0, T},
   PlotStyle → Hue[0.6], Frame → True,
   FrameLabel -> {"Test Time", "Exact MTBF"},
   PlotRange → {0, 1.25 Max[Mean[ρ∞[t]]]},
   GridLines → Automatic, DisplayFunction → Identity];
Show[{Actual, Exact, Finite, Inf, LC}, DisplayFunction -> $DisplayFunction];
```

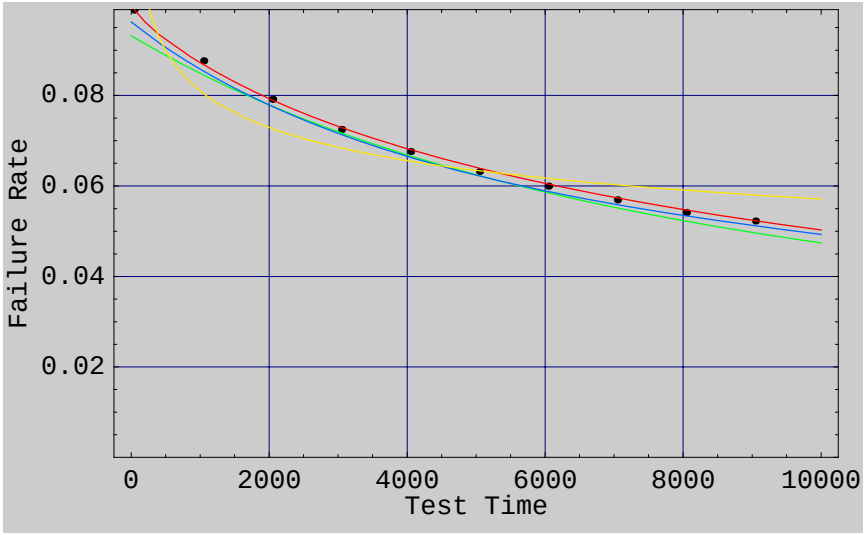

Figure 18. System Failure Intensity.

A.10 The Rate of Occurrence of Unseen Failure Modes.

In this section the rate of occurrence of unseen, or unobserved, failure modes (i.e. h[t]) is studied. Figure 19 below shows a plot of h[t] over a test period of 10,000 hours. This quantity is important since it reveals the portion of the system failure intensity that has not yet been observed. There are three series shown in Figure 19. The red line is the expected rate of occurrence of new modes. The green line is the PM2 estimate of the rate of occurrence of new modes for finite k, and the blue line is the PM2 estimate of the rate of occurrence of new modes as $k \rightarrow \infty$.

```
(*** EXACT - RED LINE *)
Exact = Plot[Mean[hE[t]], {t, 0, T},
   PlotStyle → Hue[1], Frame → True,
   FrameLabel -> {"Test Time", "h[t]"},
   PlotRange → All, GridLines → Automatic,
   DisplayFunction → Identity];
(*** FINITE - GREEN LINE *)
Finite = Plot[Mean[hK[t]], {t, 0, T},
   PlotStyle → Hue[0.35], Frame → True,
   FrameLabel -> {"Test Time", "h[t]"},
   PlotRange → All, GridLines → Automatic,
   DisplayFunction → Identity];
(*** INFINITE - BLUE LINE *)
Inf = Plot[Mean[h∞[t]], {t, 0, T},
   PlotStyle → Hue[0.6], Frame → True,
   FrameLabel -> {"Test Time", "h[t]"},
   PlotRange → All, GridLines → Automatic,
   DisplayFunction → Identity];
Show[{Exact, Finite, Inf}, DisplayFunction -> $DisplayFunction];
```

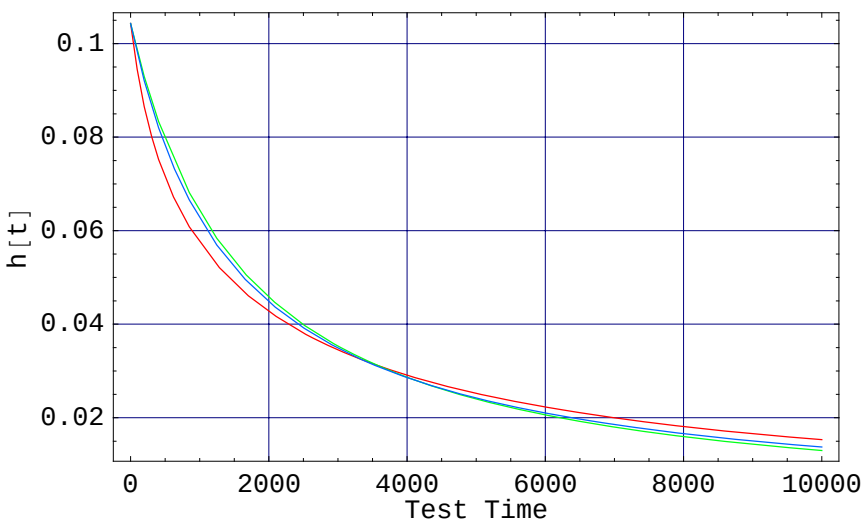

Figure 19. System Failure Intensity due to Unobserve Modes.

A.11 System MTBF based on Planning Parameters.

We revisit the system MTBF in order to construct the MTBF curves from planning parameters. The black dots represent the actual system MTBF which is known since the failure rates are simulated. The red line is the reciprocal of the expected system failure intensity. The green line is the PM2 estimate of the system MTBF using a finite number of modes, and the blue line is the PM2 estimate of the MTBF for an infinite number of modes. The yellow curve is the esimate of the system MTBF provided by the AMSAA-Crow model. In Figure 20, the series are not statistically fitted like the MTBF curves previously shown in Section A.8. In this case, the series are generated directly from planning parameters. In particular, the initial MTBF, and the goal MTBF were chosen as the realized values obtained during the simulation replications.

```
(*** ACTUAL - BLACK DOTS *)
ActualFR = Table[
   FailureRateData = {};
   Table[
    SurfacedModes = Position[ReplicatedFOT[[i]], _?(# ≤ t &)];
    m = Length[SurfacedModes];
    ρ = Sum[((1 - Extract[ReplicatedFEF[[i]], SurfacedModes][[j]])
          Extract[ReplicatedFailureRates[[i]], SurfacedModes][[j]]) +
        Sum[Delete[ReplicatedFailureRates[[i]], SurfacedModes][[j]], {j, 1, k_B - m}], {j, 1, m}];
    AppendTo[FailureRateData, ρ];
    , {t, 0, T, 1000}];
   FailureRateData, {i, 1, Replications}];
AverageActualFR = Mean[ActualFR];
Actual = ListPlot[Transpose[{steps, 1 / AverageActualFR}],
   Frame → True,
   FrameLabel → {"Test Time", "MTBF"},
   PlotRange → {0, 1.25 Max[1 / AverageActualFR]},
   GridLines → Automatic,
   PlotStyle → PointSize[.015],
   Background → GrayLevel[0.8],
   DisplayFunction → Identity];

(**** PM2 *)
ActualMGs = Last[Transpose[1 / ActualFR]];
β∞ = Map[1/T ((1 - 10/#)/(.8 - (1 - 10/#))) &, ActualMGs];
βk =
  Map[(x /. FindRoot[1/((1 + x T)^(0.1/(k_B x) + 1)) == 1 - (1/0.8) (1 - 10/#), {x, β∞}])[[1]] &, ActualMGs];
```

```
pK = 0.1/(kB βk);
hK[t_] = 0.1/(1 + t βk)^(pK+1);
ρK[t_] = (1 - 0.8) (0.1 - hK[t]) + hK[t];
ρE[t_] = Table[
   λB = ReplicatedFailureRates[[i]];
   dB = ReplicatedFEF[[i]];
   {Sum[(1 - dB[[j]]) λB[[j]], {j, 1, kB}] + Sum[dB[[j]] λB[[j]] e^(-λB[[j]] t), {j, 1, kB}]},
   {i, 1, Replications}];

(*** CROW *)
βcrow = Map[x /. FindRoot[1 / Eλ_{A,K} == T (Gamma[1 + 1/x]) / (T/(x #))^(1/x), {x, 1}] &, ActualMGs];
λcrow = T^(1-βcrow) / (βcrow ActualMGs);
ρcrow[t_] = λcrow βcrow t^(βcrow-1);

(*** PLOTS *)
p1 = Plot[
   {Mean[1 / ρE[t]],
    Mean[1 / ((1 - 0.8) (0.1 - 0.1/(1 + t * β∞)) + 0.1/(1 + t * β∞))],
    Mean[1 / ρK[t]],
    Mean[1 / ρcrow[t]]}, {t, 0, T},
   PlotStyle → {Hue[1], Hue[0.6], Hue[0.35], Hue[0.15]},
   Frame → True,
   Background → GrayLevel[0.9],
   FrameLabel -> {"Test Time", "Exact MTBF"},
   PlotRange → {0, Max[ActualMGs]},
   GridLines → Automatic,
   DisplayFunction → Identity];
Show[{p1, Actual}, DisplayFunction → $DisplayFunction];
```

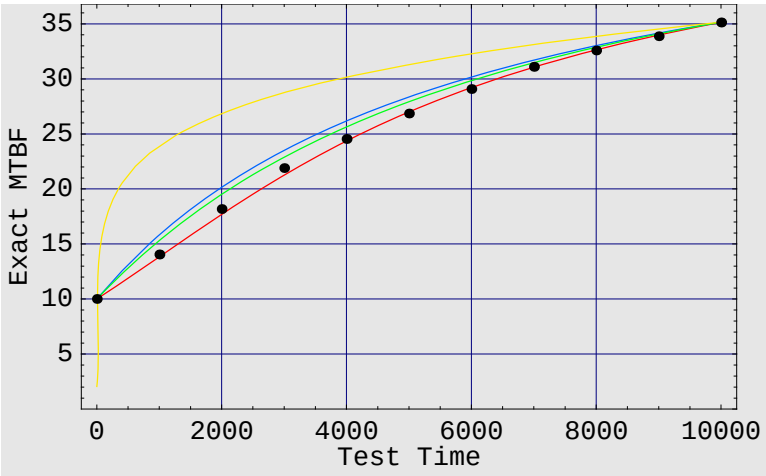

Figure 20. System MTBF based on Planning Parameters.

APPENDIX B - DISTRIBUTION LIST

THIS PAGE IS INTENSIONALLY LEFT BLANK.

DISTRIBUTION LIST

No. Copies	Organization
6	U.S. Army Research, Development, and Engineering Command U.S. Army Materiel Systems Analysis Activity AMSRD-AMS-LA; ATTN: J. Brian Hall 392 Hopkins Road Aberdeen Proving Ground, MD 21005-5071
1	Defense Technical Information Center ATTN: Raji Bezwada (OCA) 8725 John J. Kingman Road, Suite 0944 Fort Belvoir, VA 22060-6218
4	U.S. Army Research, Development, and Engineering Command Director; U.S. Army Evaluation Center CSTE-AEC-RAM (ATTN: Steve Yuhas) 4120 Susquehanna Avenue Aberdeen Proving Ground, MD 21005-3013
2	Office of the Secretary of Defense Acquisition Logistics and Technology; Defense Systems; Systems Engineering; ATTN: Peter Nolte 1851 S. Bell Street; Crystal Mall 3, Suite 104 Arlington, VA 22202
1	Office of the Secretary of Defense; Program Assessment and Evaluation Room BE779; ATTN: COL D. Mark Husband 1800 Defense Pentagon Washington, DC 20301-1800
1	Institute for Defense Analysis Operational Evaluation Division ATTN: Dean DeWolfe 4850 Mark Center Drive Alexandria, VA 22311